**Hugo Cardoso
Da Cruz**

Desenvolvimento de elétrodos em substratos poliméricos flexíveis para biossensores orgânicos

Development of electrodes in polymeric flexible substrates for organic biosensors

**Hugo Cardoso
Da Cruz**

Desenvolvimento de elétrodos em substratos poliméricos flexíveis para biossensores orgânicos

Development of electrodes in polymeric flexible substrates for organic biosensors

Dissertação apresentada à Universidade de Aveiro para cumprimento dos requisitos necessários à obtenção do grau de Mestre em Engenharia Física, realizada sob a orientação científica do Professor Doutor Luiz Fernando Ribeiro Pereira, professor auxiliar do Departamento de Física da Universidade de Aveiro.

Dedico este trabalho aos meus pais e irmã.

o júri

presidente

Prof. Doutor Manuel Almeida Valente
professor associado da do Departamento de Física da Universidade de Aveiro

arguente

Prof. Doutor Senentxu Lanceros-Méndez
professor associado do Departamento de Física da Universidade do Minho

orientador

Prof. Doutor Luiz Fernando Ribeiro Pereira
professor auxiliar do Departamento de Física da Universidade de Aveiro

agradecimentos

Antes de mais quero endereçar os meus maiores agradecimentos ao meu orientador Professor Doutor Luiz Fernando Ribeiro Pereira e ao meu orientador no âmbito empresarial Eng. João Gomes, pela oportunidade única que me deram de trabalhar neste projeto e por toda a disponibilidade e compreensão demostradas ao longo de toda a realização do mesmo.

Durante toda a realização do projeto em âmbito empresarial, no CeNTI, tive a felicidade de ser acompanhado pelo Eng. André Pinto, que me deu uma incansável e fulcral ajuda. Agradeço toda ajuda e conselhos e ensinamentos transmitidos, não só a nível do projeto em si mas também noutras áreas.

Um especial agradecimento ao António Marques pela disponibilidade demonstrada, mesmo em momentos de muito trabalho, para realizar toda a impressão em slot die e também pelos conselhos dados durante o trabalho.

A todos os colaboradores do CeNTI, endereço um agradecimento também pela forma como me receberam e pela disponibilidade demonstrada para ajudas pontuais ao longo do trabalho.

Ao longo de todo o estágio, tive a oportunidade de partilhar espaço, ideias e momentos importantes com um grupo fantástico de estagiários do CeNTI, que demonstrou sempre uma interajuda e um enorme espirito de grupo que facilitou imenso, não só a integração de todos na empresa, mas também o desenvolvimento de todo o projeto. Sem querer individualizar, um obrigado especial a este grupo.

Um obrigado ao grande espírito de camaradagem demonstrado mais uma vez pelo meu colega e amigo Pedro Gouvinhas, que me acompanhou durante toda esta "aventura" em Vila Nova de Famalicão, e que me prestou uma grande ajuda na realização de todo o trabalho sempre que necessitei.

A todos os colegas, amigos e professores com os quais tive o prazer de conviver, trabalhar e aprender ao longo de todo meu percurso académico.

E finalmente, o agradecimento mais especial e importante de todos, que quero endereçar há minha família, pois sem o seu apoio a vários níveis nada teria sido possível. E também a uma pessoa especial, Agnieszka Bajor, pela paciência demonstrada para me aturar mesmo a 3000 km de distância e pela ajuda a nível linguístico que com certeza melhorou a qualidade de todo o trabalho.

palavras-chave

Sensores orgânicos, eletrónica impressa, biossensores de odor, nariz eletrónico, polímeros condutores, screen printing, slot die, PEDOT:PSS.
.

resumo

O desenvolvimento de eletrónica orgânica e consequentemente o desenvolvimento de sensores baseados em polímeros orgânicos, atraíram a atenção da comunidade científica. Motivada pela multifuncionalidade, fácil processamento e baixo custo destes materiais, novos biossensores de odor para diversas aplicações começaram a ser desenvolvidos, incluindo na área médica, para a deteção de doenças.

Este trabalho, baseou-se no processo de "scaling-up" de um trabalho prévio que teve um objetivo meramente laboratorial, em particular no desenvolvimento de biossensores orgânicos de odor (conceito de nariz eletrónico), baseados em polímeros orgânicos (PEDOT:PSS) num paradigma pré industrial e fabricados pelo meio de técnicas de impressão de eletrónica orgânica, tais como screen printing e slot die. Foram desenhados novos microelétrodos de carbono com diferentes parâmetros geométricos que foram posteriormente produzidos por screen printing. Através da técnica de impressa de slot die, foram posteriormente impresso filmes de PEDOT:PSS sobre os microelétrodos.

Após o processo de fabrico, os sensores foram morfologicamente caraterizados por microscopia ótica, microscopia de força atómica, perfilometria e eletricamente caraterizados através da técnica de duas pontas. Os sensores foram testados para diferentes analitos, nomeadamente para dois analitos ginecológicos. A resposta resistiva e capacitiva dos sensores expostos aos analitos, foi obtida e analisada, com especial atenção na influência dos parâmetros geométricos dos microelétrodos de carbono e também na espessura do polímero. Por fim, os sensores foram também testados para outros analitos compostos por queijo azul.

keywords

abstract

The increase of organic electronics and consequently, the development of sensors based on organic polymers have attracted a lot of attention of the scientific community. Intrigued by these multifunctional, easily processed and low cost materials, it has started to develop odour biosensors for different applications, including medical field and the detection of various diseases.

The present work, is focused in the scaling-up of a devoted laboratory approach, in particular concerning the development of organic odour biosensors (electronic nose concept) based on a conductive polymer (PEDOT:PSS) in a pre-industrial approach and produced by means of electronic printing techniques, such as screen printing and slot die. New carbon microelectrodes with different geometrical parameters were designed and processed by the screen printing technique. Further, the slot die technique was applied in order to print the PEDOT:PSS film over the microelectrodes.

After the fabrication process, the sensors were morphologically characterized by optical microscopy, atomic force microscopy, profilometry and electrically identified by the two points probe method. The sensors were tested with the use of different analytes with the main focus on two gynaecological analytes. The resistive and capacitive electrical sensor responses for the analytes were analysed and discussed in depth. Important results were obtained with regard to the influence of the geometrical parameters of the carbon microelectrodes and also to the polymer thickness. Finally, the tests on the sensors were also carried out with the use of other analytes which contained blue cheese.

Contents

List of Symbols

A

B

C

D

E

F

G

H

I

L

M

N

O

P

List of Tables

List of Figures

1.   Introduction

1.1.   Context and aim of the project

In the past decades we witnessed a big development in sensor technology which have changed completely the way we interact with electronic devices and consequently, it has transformed our lifestyles. Both, the influence of this type of technology on our lives and a wide range of possible applications motivated the academic community to develop new sensor materials and methods which not only have improved the performance of the older technology, but also gave us the possibility to solve new problems and to look forward for new and more complex challenges.

One promising application of sensors concerns medicine. Therefore, a lot of efforts have been undertaken to devise new bio- and chemical sensors which can be applied in medical devices in order to detect microorganisms that may be detrimental to our health. This type of technology is very important for physicians not only to diagnose potential diseases their patients may suffer from, but also to evaluate the evolution of diseases and the efficacy of medical treatment. Diagnostic medical devices normally have still a high associated cost, and nowadays medical community seeks for the development of new cheaper and non-invasive devices which can be used for real time detection.

Some bio- and chemical sensor devices are able to detect and distinguish groups of different chemical elements associated with specific diseases. One of these are electronic noses. New e-noses were designed and developed in order to reach medical device standards Conductive polymer (CP) properties, as a gas sensor, make them a good choice for the development of cost-effective and transportable e-noses, which can be even operated remotely.[1]. Although there are already a couple of commercial e-noses on the market based on conductive polymers, they still have a big cost associated, and currently there is still a big research in order to improve their performance, especially considering the big exigencies for the development of medical devices. In the medical field, there is an ongoing big research in order to test several commercial e-noses for the detection of several diseases [2].

This project has been planned following the results of a previous thesis work done by Maria Isabel a Marques entitled *"Odor Biosensors for the detection of gynecological pathologies"* [3]. In the previous work, the study relied on the development of flexible CP based odor sensors using PEDOT:PSS as sensing material, deposited in a PET substrate by spin coating, for the detection of vaginal candidiasis, a common fungal vaginal infection. Promising results were obtained, since it was possible to detect by resistive and capacitive electric response analysis, an analyte based on a fungal culture of this disease.

Based on the promising results obtained, a new challenge of studying the possibility to develop a medical device emerged. The challenge remains in scaling up approach when developing these type of sensors with a pre-industrial procedure in the future. Consequently, the objective for the present work is to develop new sensors using a roll to roll process in order to create a large number of sensors. Therefore, a new procedure was adjusted for the materials and the facilities available. All the steps of the development and fabrication of this sensors were tested and optimized.

First, new interdigitated microelectrodes, with different geometrical parameters and shapes were designed in order to obtain information about the influence of different geometrical parameters in the sensors performance. New interdigitated carbon microelectrodes were printed with the use of the Screen Printing technique, several times until the process was optimized. The Slot Die printing technique was used as the roll-to-roll process to print out different films of PEDOT:PSS over the carbon microelectrodes. This process was also tested and optimized.

A new experimental setup was also developed and notwithstanding the failure, new suggestions of improvement for the future were planned.

1

In the end, the microelectrodes were used as resistive and capacitive sensors. Their sensorial response was characterized by two different gynecologic analytes. Other analytes as alcohol, acetone and blue cheese were also used in order to obtain more information about the sensor sensitivity and potential for their application in different fields.

In sum, main objective was to evaluate the performance and the potential of this type of sensors developed with a new methodology, especially, for their application in gynecological pathologies and also to characterize qualitatively their electrical responses.

The project was developed in cooperation with CeNTI (Centre for Nanotechnology, Smart Materials and Systems [4] during traineeship.

1.2.   Biosensors and chemical sensors

1.2.1.   Introduction

The observation of biological systems gave us the hint how to develop technology able to mimic different organisms and specially their capability of discovering and responding to several different chemical and physical stimuli. The use of these intrinsic sensing properties of living beings, used to detect other biological systems, opened the door for the development of new technology able to observe life. Therefore, a lot of attention has been paid to the development of biosensors which by definition, are able to detect a biologic stimulus by means of bio receptors such as cells, enzymes etc. In this piece of art, we also consider as biosensors devices which can detect a biologic stimulus produced by a biologic system, but not necessarily by means of a biologic receptor[5].

In this way, chemical sensors used to detect a biologic stimulus can be consider as a type of biosensors, since they can reveal the presence of specific chemical compounds originated from certain bio organisms. With these types of sensors, it is possible to characterize a specific environment constituted by one or a group of microorganisms, which is very useful in many applications, including biomedical devices identifying several diseases[5].

Chemical sensors can be divided into different classes according to their transducing principle and design, such as electrochemical, optical, electric, chemiresistive, chemicapacitive etc[6].

1.2.2.   Gas & liquid sensors

Chemical sensors can analyze samples in liquid and gaseous phases. The working principles of both of liquid sensors and gas sensors are quite similar, and are based on the modification of their sensing material physical properties (electric, morphologic, optic), in the presence of different chemical compounds. The materials and the configuration of these sensors can be different since the characteristics of a liquid or a gaseous environment are also different. In the end, a gaseous sensor is an electronic device which is able to "smell" gases, and a liquid sensor is an electronic device which is able to "taste" liquids. Because of this intuitive comparison between these electronic mechanisms and the biological olfactory and gustatory mechanisms, chemical sensor devices constituted by an array of gas or liquid sensors are often called electronic noses or electronic tongues, respectively.[6]

1.3.   Electronic noses & Applications

1.3.1.   The Odor and the odorants

Odor can be simply described as "the perception of smell"[7]. Odor can originate from one or a group of odorants or aromas which due to their chemical differences, cause a different sensation of smell. Odorants are volatile chemical compounds with low molecular weight (less than 300 ppm), and can vaporize completely or partially at room conditions (pressure, temperature)[8], [9]. Most of these

volatile compounds are organic and they form the so-called group of VOCs (volatile organic compounds), but not all of the odorants are organic, as it is the case of fluorine or sulphur [9].

Odorants interact with the olfactory system and produce a specific "smell print". Normally, a "smell print" is not constituted by only one odorant but by a group of odorants. Therefore, odor classification is extremely dependent on the human ability to sense and evaluate odorants. Humans are able to distinguish about thousands of different compounds from their odor. Odors can be classified according to the type of sensation they originate from, and Henning classified them in 6 primary odor classes: putrid, fragrant, ethereal, spicy, burned and resinous [7].

1.3.2. Working principle

An electronic nose, most often simply called e-nose, is a device based on a mammalian nose and as a result, is able to detect and discriminate odors[10][11]. In this sense, we can say it is a device designed to "smell". E-noses can sometimes be referred to as artificial noses, mechanical noses, odor sensors, aroma sensors, electronic olfactometry[11].

The sense of smell is one of the most important senses for humans and also one of the most complex ones. It plays an important role in our physical and social behavior and it provides us with the capability of reacting and adapting to several kinds of different stimuli which can be connected to comfortable and uncomfortable environments. Researchers concluded that 1% of the human genome is dedicated to olfaction, which clearly suggests the importance of this sense in the human evolution[12].

This complexity makes the olfactory sense very difficult to mimic when compared with other mammalian senses like vision and audition. Figure 1.3-1, shows the configuration of a human olfactory system and an e-nose.

Inside the humans' nasal cavity, the olfactory epithelium is constituted by several millions of receptor cells [13]. It is the interaction between the nasal epithelium and the odor that is responsible for the creation of the sensation of smell. Receptor cells are specialized proteins which connect only to certain types of molecules and which are connected to nervous terminations called cilia. Each protein is sensible to several different molecules and in the same way, each molecule can connect to several different proteins. Like that, the olfactory system does not discriminate odors by strict selectivity of receptor cells to a specific molecule or component, but by having a big quantity of cross sensitive receptor cells which in the end, transmit to our olfactory lobe, a big amount of data that the brain is able to process and memorize [7]. Our reaction to a certain type of odor is connected to our experience with the environment connected with it. The brain memorizes the odor creating a kind of data base, and when we are exposed again to the same type of stimulus, it creates a sensation which can be pleasant or unpleasant according to the experience we had before towards this odor and which we already know it's correlated with something positive or negative.

E-noses have a very similar working principle (see Figure 1.3-1). The detection of the odor is done by a specific sensing material. The sensing material's properties are modified by the interaction between the material and the components of the odorant gases. These properties' modification can be measured and compared with a reference environment and then further evaluated.
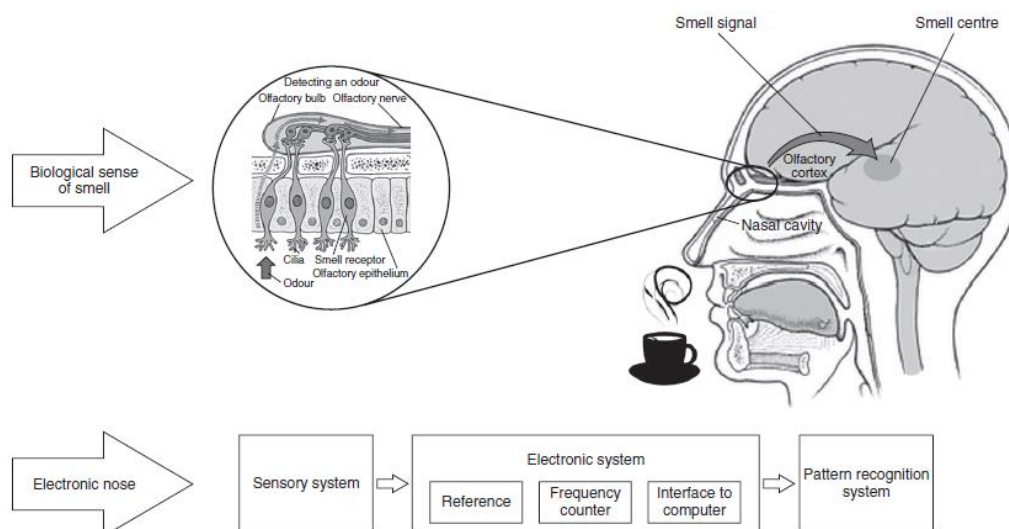
Figure 1.3-1 - Human nose and e-nose schematic comparison[11]

Normally, e-noses comprise of an array of chemical sensors with different sensibilities to the chemical components of odorant gases. The number of sensors used in array depends on the desired selectivity of the device to develop. Increasing the number of sensors normally leads to an increase in selectivity. Like olfactory receptors, chemical sensors used in the array of sensors are not developed to sense a specific component or molecule, otherwise a device would need thousands of different sensors. The number of sensors normally used in an e-nose can vary between 3 or 4 to 100 [13]. The more each of the used sensors is sensitive to only a one specific element of the odorant, the more selective is the e-nose. Even with a great number of chemical sensors, it is not possible to develop an e-nose with the same sensing performance of the human olfactory system, which has an "array" of about 100 million sensors and which is in average able to discriminate around 5000 different odors [14]. Despite of this issue, nowadays, it is possible to develop devices which are designed to have selectivity to a specific group of chemical components and discriminate them [15].

After being detected by the array of sensors, the response from each sensor needs to be measured and then converted into signal. This is solved by the use of specific electronic circuits typically used in sensor devices as voltage dividers and Wheatstone bridges. The type of these interface circuits needs to be chosen according to the type of chemical sensor used in the array. Then analogic electrical signals need to pass through a unity of signal conditioning in order to be processed by a computer. Signal conditioning circuits are based on buffering, amplification, filtering and also other special features. After that, the signal is ready to be converted into digital data, processed, and finally analyzed with the use of specific mathematic methods[16].

Signal processing is a very important step which can have a considerable influence on the performance of the device. The main objective of processing the digital signal is to filter the important part of the signal and extract it in order to be further analyzed. This methods of processing include baseline manipulation, signal compression and normalization[16].

Data that e-noses provide can be very complex. Instead of providing specific information about the nature of compounds, these devices produce a kind of "fingerprint" or "smellprint" which is the result from a mixture of multiple components. Consequently to process and analyses this data, the use of complex mathematical methods is needed[17].

There are several multivariate methods that are normally used to perform data analysis in e-noses. Their use depends mostly on the desired accuracy of the results and on the type of samples the device is going to analyse. These methods don't provide specific results about the presence or the

4

absence of certain elements, but by using them we can obtain a multivariate description of the samples which identify patterns between samples. Therefore, in this kind of devices a subset of multivariate analysis defined as pattern recognition methods (PARC) is used[17].

Pattern recognition methods can be divided and organized in several ways. One way is to divide them by statistical and biological based methods and also by supervised and unsupervised methods. Examples of statistical methods, are the most commonly used Principal component analysis (PCA), partial least square (PLS), multiple linear regression (MLR), principal component regression (PCR), cluster analysis (CL) or linear discriminant analysis (LDA). Examples of biologically based methods are neuro network methods (ANNS), also often called neuro-machines like ANN or SOM, or Fuzzy methods as fuzzy inference systems (FIS) and adaptive resonance theory (ART)[17].

Unsupervised techniques are more useful when there is no prior information about the chemical composition of the odorant. Supervised techniques have the objective to mimic the learning ability of human brain, and provide machine learning capabilities. These are also able to include parameters such as temperature or humidity in the calculations[17].

1.3.3. Different types of E-noses

E-noses can be differentiated by their sensing technology. There are different technologies used to construct them. These technologies differ in the kind of material used and also in the transducing principle. Taking into account the transducing principle, e-noses can be evaluated as potentiometric, amperometric, conductmetric, gravimetric, capacitive, calorimetric, optical, resonant or even fluorescent [18].

Normally these devices are divided according to the sensing material or design. Therefore the main classes of electronic noses are: Metal oxide Semiconductors (MOS), Metal oxide Semiconductors field effect transistors (MOSFET), conductive polymers (CP), piezoelectric and optical.

Metal Oxide Semiconductors –MOS:

MOSs sensors were the first to be developed and commercially used. A metal oxide semiconductor layer changes its electrical resistance after the adsorption of gas molecules. Normally used N-type metal oxide semiconductors are tin dioxide, zing oxide, titanium dioxide or iron (III) oxide, and commonly used p-type MOS are cobalt oxide or nickel oxide. Due to reproducibility of the manufacture process, thick film technology is normally used in these sensors, even if thin films offer shorter time responses and better sensitivity. Changes in resistance/conductance rely on the oxidation of the sample compound by the semiconducting layer. However, in order to observe this phenomena, sensors need to work at a temperature of 250ºC up to 450ºC and thus, the use of an heating system together with the sensor is needed, which increases the complexity and the cost of these devices.[13], [19], [20].

Metal Oxide Semiconductor Field Emission Transistors MOSFET:

They are widely used specially due to their working system simplicity. Those kind of transducers have exactly the same structure of a typical MOSFET, but in these case the gate is made of gas sensitive catalytic metal like platinum (Pt), palladium (Pd) or iridium (Ir). Gaseous compound react with the catalytic metals which modifies the surface-charge density and consequently the potential of the device. This devices measure the change of potential needed to keep the drain current constant. MOSFETs selectivity and sensitivity can be increased by changing the operating temperature. However this kind of sensor in order to achieve good quality has a high cost of manufacturing. [13], [19], [20].

Piezoelectric:

These gas sensors are based on the changes of the resonant frequency of a piezoelectric disk when exposed to VOC's. These materials have a specific resonant frequency. When they are stimulated at this frequency and further exposed to an odorant, gas molecules are adsorbed on their structure and their mass changes which consequently leads to a reduction of their resonant frequency. The reduction

is proportional to the mass of the odorant compounds which allows them to be identified according to the magnitude of resonant frequency variation. There are two types of piezoelectric gas sensors, called BAW (bulk acoustic wave) and SAW (surface acoustic wave). Piezoelectric materials used in these devices are quartz, lithium niobate (LiNbO3), or lithium tantalite (LiTaO3).[7] [9] [10]

Nanostructured materials:

In the recent years the progress in e-nose technology lead to the development of new gas sensors based on nanostructured materials such as Metal based nanostructures, MOS based nanostructured, carbon black, CNTs (Carbon nanotubes), graphene and other carbon based nanomaterials and also nanocomposite materials such as polymer based composites, and metal oxide based composites[22]–[27]. Carbon based nanomaterials, have already been widely used in chemical gas sensor studies, including in the development of system on chip devices[28]. These materials offer a big sensing area/volume ratio and their structure can be manipulated to enhance sensitivity and selectivity[25].

All of these new materials are a promising approach to the development of more sensitive and selective chemical sensors, which can reduce the number of sensors used in an electronic nose and amplify the range of applications of these devices. However most of these materials are still being used in laboratory sensors and there is still a long path to follow in order to reach commercial applications.

1.3.4. Applications

E-noses are an emerging type of technology and nowadays, they are already applied in many fields of study and are expected to reach in the future a level of performance which will allow their implementation in new fields.

Even though these devices have a huge versatility and they have been already produced for commercial reasons for more than two decades, most of their applications are still in laboratory stage. Examples of fields of their application include the biomedical industry, alimentary industry, environmental study and monitoring, security systems, cosmetic industry and also aerospace and automotive industry.

The Table 1.3-1, summarizes some of the fields of application and also some of the different analysis done by e-noses for each field.

6

Table 1.3-1 – Applications of electronic noses.

Field of Application	Type of Analysis
Biomedical[2], [29]–[32]	Human Breath (Ex: detection of diabetes, pneumonia, lung cancer etc)
	Genetic testing (Presence of genetic anomalies/disorders)
	Bacteria cultures studies
	Colorectal cancer
	Bacteriologic vaginosis
	Human Fluids like Blood, urine and sweat (identification of specific pathogenic agents in fluid samples)
Alimentary[32]–[37]	Food spoilage and quality
	Beverage spoilage and quality (Ex: Wines, juices, milk etc)
Environmental[31], [38]–[40]	Air pollution monitoring
	Water quality monitoring
	Soil analysis
	Medical environment monitoring
Security [13], [31], [41]	Detection of explosives and Chemical warfare agents (CWAs)
	Prevention of dangerous gases (Sarin, Soman etc)
Cosmetic[31], [42]	Skin, body and hair cosmetic products
Aerospace[31], [43]	Shuttles air monitoring
Automotive [31], [43], [44]	Monitoring combustion efficiency
	Monitoring cabin air

1.4.   Conductive polymer based e-noses

1.4.1. Conductive polymers

Conductive polymers, often called synthetic metals, as the name suggests, are a kind of materials which conjugate the structural properties of a polymer with electric proprieties typically found in metals/semiconductors.

In 1977 an intrinsic conductive organic polymer of polyacetylene doped with iodine was syntethized by Alan J. Heeger, Alan MacDiarmid and Hideki Shirakawa. The good conductivity observed in this material comparable to that found in some metals or carbon fibers, called the attention of the scientific community, who started to explore CP's properties for the development of different type of devices. Active layers of gas sensors made of CPs started to be reported in the 80's [45][46].

Intrinsic conductive polymers form a conjugated system of alternated single and double carbon bonds. In these systems, a chemical binding with sp^2pz configuration leads to the overlap of atomic orbitals and consequently to a delocalization of a π electron cloud along the backbone of the polymer. This delocalized electron "cylinder" forms a path for conductivity along the polymer's backbone [45]–[48]. In the Figure 1.4-1, a polyacetylene backbone is described and it's possible to see the overlapping of the sp^2 orbitals which are bonded by a σ-bond and the decentralized π-bonds which form the "cylinder" pathway along the polymer's backbone [46].

There are several types of polymers which show conductive properties and which are widely used in gas sensor applications, like poly(acetylene)s, poly(pyrrole)s, poly(thiophene)s, poly(terthiophene)s, poly(aniline)s, poly(fluorine)s, poly(3-alkylthiophene)s, polytetrathiafulvalenes, polynaphthalenes, poly(p -phenylene sulfide)s, and poly(para -phenylene vinylene)s [45]–[48].

In their undoped state CPs don't exhibit good conductivity properties and to do so, they first need to be doped by specific elements, like it's normally done in a semiconductor. Like other polymers,

CP's can be easily manipulated in order to have a big range of properties, and particularly by doping them, we can increase their conductivity in several orders of magnitude. The highest conductive polymer is the polyacetylene which can achieve a conductivity of around $1e^4$ S/cm^2 [45]–[47].

The main characteristic which distinguish CPs from other polymers, it's their ability to exhibit good electric conductivity after being doped. The process of doping is done by oxidation and reduction reactions or as well by a process of protonation and deprotonation, which is in general particularly exhibited by polyaniline. Doping is done by the addition of both n-type (Na, K, Li, Ca, tetrabutylammonium), or p-type dopants (HCl, FeCl$_3$, HBF$_4$, BF$_3$, AsF$_6$, NaCl, I$_2$, Br$_2$, H$_3$PO$_4$, HClO$_4$, R-SO$_3$H, CH$_3$SO$_3$H, CF$_3$COOH) [45], [46]. The oxidation/reduction by the introduction of a dopant, removes/adds electrons to the polymer which leads to the generation of the so called polarons and bipolarons which will act as charge carriers. For degenerate conductive polymers instead of the formation of polarons and bipolarons, the conduction is mediated by the formation of solitons[45]–[47].

One of the main particularities of these materials is the high reversibility of their redox behavior. This means that their doped state can be completely reversed by the compensation of the charge carriers[47].~

sp² orbital σ bond   p$_z$ orbital   π bond
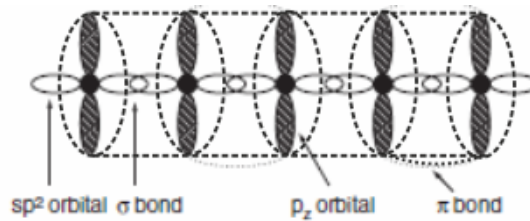
Figure 1.4-1 - Chemical structure of trans-polyacetylene [(CH)2]. Orbital diagram of the carbon backbone.(Adapted from [45]).

1.4.2. Sensing principle

Apart from the particular elevated electric conductivity which is essential for their applications in chemical sensors, the main characteristic which is responsible for their wide use in gas sensing is their high reversible redox behavior [47], [49].

Like it was already mentioned, conductive polymer's physical properties are strictly dependent of their doping level. Moreover, they can react chemically with gases at low temperatures. The interaction between CP's and gaseous analytes is mainly dependent of the absorption or adsorption (1.4-1) and desorption (1.4-2) of the molecules of the gases and the physical and chemical interactions that these gases have with the polymer. Most of the polymers react by means of redox chemical reactions with the analytes. In the common cases, a p-type CP in the presence of electron donor receives its electrons which will decrease the conductivity of the polymer.

However, in some special cases the inverse scenario seems to happen. For example, a p-type CP, like PPy, in the presence of a an electron donor like Amonia (NH$_3$), receives electrons increasing its charge carriers and consequently enhancing its hole conductivity. The opposite process happens when a CP is exposed to an electron donor, however this mechanism still needs to be studied in more detail since there are some cases where this tendency is not observed [47].

$$PPy^+ + \ddot{N}H_3 \rightarrow PPy^o + NH_3^+ \quad Adsorption \tag{1.4-1}$$

$$PPy^o + NH_3^+ \rightarrow PPy^+ + \ddot{N}H_3 \quad Desorption \tag{1.4-2}$$
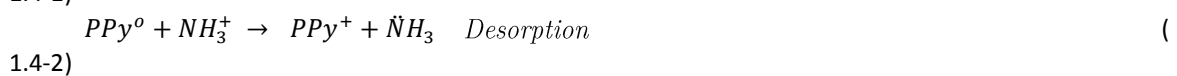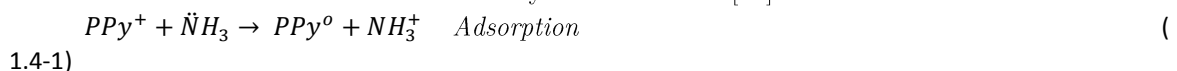
Due to the high reversibility of these redox behavior, when a CP is removed from the analyte contact, a desorption will take place and the conductivity of the CP will return to the exactly same reference value [47].

Furthermore, CP's react also with analytes by means of weak physical interactions. However, as it is the case of the chemical reactions, these mechanisms still need to be better understood. When a CP adsorbs the gas molecules, it swells. Swelling process expands the polymer's structure, thereby decreasing its conductivity. This process has especially a great influence on polymer-based composite sensors where the expansion of the polymer matrix has a major impact on the gas detection. Weak physical interactions are very important for the detection of some VOCs like toluene or benzene and some alcohols, since at room temperature they are not able to react chemically with the polymer.[47].

One of the biggest challenges of an e-nose construction is the cross sensitivity of the sensing material to several different compounds. CP's can be modified by several mechanisms which induce specific sensitivities to groups of compounds and consequently, it leads to an improvement of the sensors selectivity. This is important since this kind of manipulation of CPs can decrease severely the number of sensors used in an e-nose. The affinity to specific compounds can be achieved by the incorporation of certain synthetic and natural receptors.[15], [49].

1.4.3. Working Principle

Polymer based gas sensors are composed by a polymer based transducer and an electronic system which is almost similar to the other type of e-noses. The transducer is constituted by an electrode made of a conductor material such as silver, carbon, gold, etc and a polymer film. This electrode has two contacts which can be connected to a voltage/current dc or ac source. Normally, these electrodes have an interdigitated design like it is shown in the Figure 1.4-2 [47], [50]. Over this electrode is deposited or printed a conductive polymer film which will act as an electric conductive path between the contacts of the electrode. Consequently, an electric field is generated between the contacts of the electrode and the current will flow (or electrical carriers are trapped at electrodes) through the polymer and the system, "microelectrode + polymer", acts as a resistance or dielectric. A fixed DC current or voltage can be applied and the resistance can easily be measured with an ohmmeter. When an AC current/voltage is applied the system can be also characterized by a capacitance[47],[51].

As it was mentioned before, the polymer is the sensing material. When it is exposed to different gases, its conductivity is modified. Therefore, the "microelectrode + polymer" acts as an electric transductor which is then connected to an electronic system capable of measuring the differences of resistance or capacitance.

The Figure 1.4-2 shows a very simplified electric circuit which can describe an organic electronic device. The conductive polymer behavior is divided by a group of three different contributions, which are connected in parallel, depending on the different types of conductivity of the polymer.
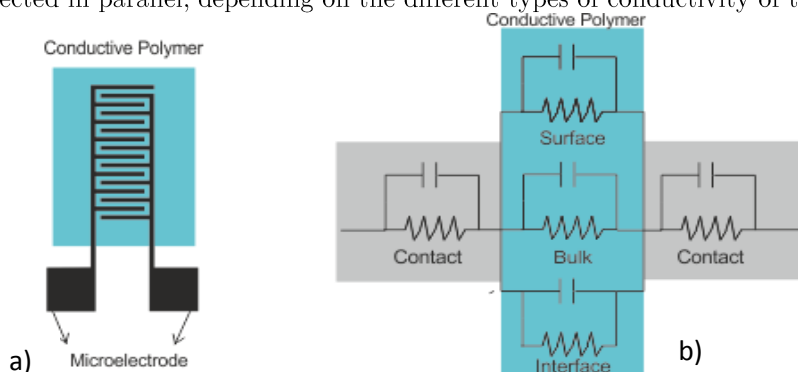
Figure 1.4-2 - Typical organic sensor device structure: a) top view of an interdigitated microelectrode with a layer of a conductive polymer deposited over the microelectrode; b) resumed electrical circuit of an organic sensor device.

9

1.4.4. Advantages & disadvantages

CP's offer good advantages when compared to other materials used in e-noses for certain applications, however they also show some disadvantages for others. Therefore, CPs are a great alternative relative to most often used materials like MOS, even if they are not meant to substitute completely the usage of these different materials.

Advantages:

Versatility/Facile property adjustment: CPs have unique electrical, mechanical and optical properties and these properties can be easily modified and tailored to specific applications by different means[20], [47], [48], [52], [53].

Easy processing: CPs can be easily fabricated when compared to other chemical sensor materials. Their good mechanical properties and the fact that they can be made soluble or insoluble make them proper to be also used in different ways. The possibility of enhancement of their solubility makes them compatible also to many different deposition techniques[20], [47], [53].

High Sensitivity: The detection limit is dependent of the type of analytes. For reactive analytes it can be lower than 1ppm and the case of inert gases, it can be up to several ppm[28], [47]. CPs show also specific high sensitivity to polar compounds.[1], [11]

Room temperature operation: Unlike MOS based sensors, CP based sensors can operate at room temperature with good signal. Therefore, CP show some advantages for simple, portable and low energy consumption devices which can be used at room temperature [2], [47].

High conductivity/weigh ratio: These property is very important for several applications especially when a small device is needed [48].

Disadvantages:

Sometimes Low selectivity: CPs show in some cases, an intrinsically low selectivity to different analytes. However like it was already mentioned they have the possibility to be modified by several different ways in order to enhance their selectivity. However it's always necessary the use of arrays of several sensors to achieve good selectivity results[20], [53].

Short life-time: CP based performances decrease considerably with their life time, especially when they are stored in air[20], [47], [53]. Studies report life times of these sensor can be from 9 to 18 months [1].

Irreversibility: One of the problems found is the lack of reproducibility of sensors performance after usage, since after cycles of tests they show some response irreversibility[47].However, due to the main purpose of this work, such question is not a problem.

Sensitivity to water vapor and moisture: Most of CPs are very reactive to water vapor. Water vapor common interferes with CPs response at room temperature, so then differences in humidity have a big influence in CP based sensors performance. Another common unwanted effect in CPs is their high sensitivity to moisture which has influence also in sensors response[20], [47], [53].

2. Materials & Methods

2.1. The Substrate

In the present work, polyethylene terephthalate (PET) was chosen as a substrate. PET exhibits very good characteristics in flexible electronics, and therefore, in flexible sensors too. It suits the desired characteristics as a substrate for our sensors. It has high mechanical, electrical and chemical resistance, it is easy to manufacture and to shape, it is a transparent, cheap material of a low density. Furthermore, PET is usually used as a flexible polymer substrate in screen printing [54].

.PEDOT:PSS

PEDOT (poly(3,4-ethylenedioxythiophene) is an intrinsic conductive polymer which was for the first time synthetized in 1988. For the last decades, this polymer has been widely studied and used in many applications such as in thin film transistors, OPV's, light emitting diodes, sensors, bioactive coatings, memories and others. One of the main reasons why PEDOT:PSS attracted the attention of the scientific community was the fact that it is available in a dispersed transparent solution, which allowed it to be deposited by many different techniques and in various substrates. However, PEDOT alone is a non-soluble and unstable polymer, and in order to be available in a dispersed solution, PEDOT needs to be conjugated with PSS[55].

PEDOT is obtained by the oxidative polymerization of EDOT (3,4-ethylenedioxythiophene). Different oxidizing agents can be used such as Iron (III), Iron (III) nitrate, Iron (III) chloromide. Yet, the most effective oxidizing reagents are monovalent peroxodisulfates' cations like sodium potassium and ammonium. Oxidants act not only as precursors of the polymerization, but also as dopants. This type of doping is sometimes defined as primary doping. During the oxidation each monomer loses two electrons and a polymer conjugated with free positive charges is created. To compensate the excess of positive charges and stabilize the polymer a counterion is needed. PSS is a bulk isolator polyanion easily soluble in water which in this case acts as the counterion to stabilize the polymer and simultaneously allows the PEDOT to be obtained in solution. After oxidizing polymerization, the polymer has one net free positive charge carrier per every 3 or 4 thiophene rings. Therefore, the PEDOT:PSS is a p-type conductive polymer in which positive charges act as the charge carriers[55].

However, in order to obtain high conductive PEDOT:PSS solutions, normally a secondary doping process is needed. Unlike the primary doping which is based on redox reactions and can be reversed, secondary doping is not reversible. Secondary dopants are chemical additives which can increase the conductivity of PEDOT:PSS by several orders of magnitude. Mechanisms for the increase of conductivity are still being studied and depend on the type of dopant. The most commonly used dopants are monovalent alcohols such as methanol and ethanol, polyols such as sorbitol, glycerol and ethylene- glycol and others compounds such as diethylene glycol, dimethyl sulfoxide (DMSO)[55].

The conductivity mechanisms of PEDOT:PSS are still poorly understood. Like in other conductive polymers, the propagations of free charge carriers along the backbone of the polymer seem not to be enough to explain the polymer conductivity. Interchain conductivity mediated by hopping seems also to be a mean of electrical conductivity for PEDOT:PSS[55], [56].

11

There are several commercial grades of PEDOT which have different optical and conductive proprieties. Several parameters can contribute to a change of grade proprieties, such as the ratio between PEDOT and PSS in the solution, viscosity and PH[57]. Different grades of high conductive PEDOT:PSS are commercialized by *Clevios*, like *PH1000* and *PH500* [57]. In the previous work, a solution of PH500 was used, and it showed very good sensing properties [58]. In the current work, since this grade of PEDOT:PSS stopped to be commercialized, a solution of the *PH1000* grade was used. This grade is more conductive than the *PH500* one and was developed to obtain high conductive polymer films. The Figure 2-1.1 shows the chemicals structure of PEDOT and PSS.
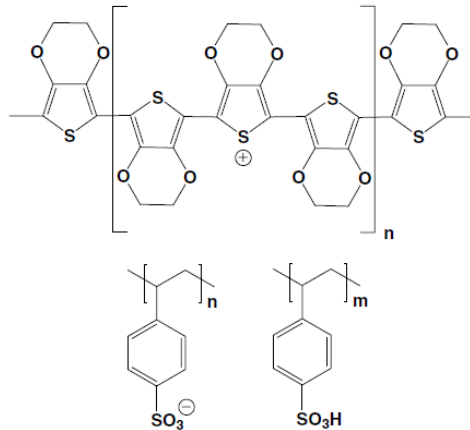
Figure 2-1.1 - PEDOT:PSS chemical structure. PEDOT in the top. PSS in the bottom.[59]

2.2.   Screen Printing

Screen Printing also known as silkscreen printing, it's a serigraphic printing technique based on a stenciling process which is widely used in graphic arts. However, thanks to its easy adaptability, this printing process is also used in many industrial manufacturing applications, including printed electronic circuit boards. Screen printing is the most mature technology in printed electronics. It is simpler, faster and more versatile than other printing techniques and it is achieved at a low cost. It can be automatized and adapted to mass and lab production and offers special advantages in non-flat objects printing.[60]–[62]

The printing process consists in forcing the ink to be transferred through a screen. The screen is a woven mesh made of silk, synthetic fibers or metals, and is affixed to a rigid aluminum or steel framework. Photosynthesized masks are drawn to form a desired image and non-image areas which constitute open and close pores for the ink respectively.[60], [61]

When the printing process starts, the mesh is initially flooded by an ink. The squeegee moves horizontally and applies a vertical force to the flexible mesh which forms an area of contact with the substrate and consequently, part of the ink is transferred through the mesh apertures and adders to the substrate. Due to cohesive forces, the viscous fluid (ink) forms a series of column shaped deposit, but with the movement of the squeegee these column shaped columns spread and form an uniform layer.[60]

Since this technique has been already used in microelectrode development and in flexible sensor manufacturing, suits low cost applications, it can be automatized and adjusted to a R2R process and consequently an industrial approach and it was also available in *CeNTI* facilities, it suits the objectives planned for the current work.

The Figure 2.2-1, shows a resume scheme of a typical screen printing device.
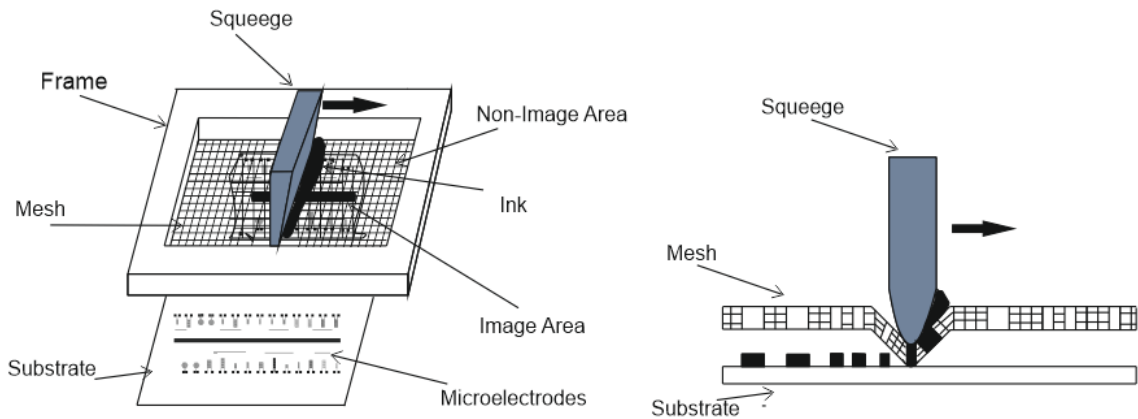
Figure 2.2-1 - Scheme of the Screen Printing technique.

2.3. Slot die deposition

Slot Die is a coating technique invented by Beguin as a fast and precise coating procedure for the manufacturing of photographic films. This technique is considered one of the most efficient coating methods for many products and it has already been applied in many advanced products such as optical films and colour filters, LCD panels, batteries, flexible printed circuits and sensor printing. The main feature of this technique is the possibility to provide a uniform coating in terms of thickness and homogeneity by defining a specific width of deposition. Slot die is available in a flatbed system and also in a R2R printing system, where the solution is poured from the top through the die and the substrate is placed below in a cylinder as it is shown in the Figure 2.3-1. [62], [63]

In this technology, the structure and geometry of the manifold plays an essential role in the deposition process. There are two types of different basic manifold designs for the slot die: the coat-hanger shape and the T-shape.[64]

The coat-hanger shaped design has a pressure compensation design with the use of a preland slot section with varying length downstream. To compensate a pressure increase in the slot die chamber, the pressure in the preland section must decrease at the same rate as it increases in the manifold section. In this type of configuration, while the coat hanger design style is fixed, other dimensions can vary according to different parameters as the die width, flow rate and coating material requirements. Coat-hanger design can be modified and adapted to specific applications taking into account particular information such as the rheology curve, flow rate, material density and processing temperatures and other special material characteristics like degradability.[64]

The T-shaped design has a constant cross-section and thus, it does not have a compensation method. This configuration has a larger manifold section with the objective of reducing the resistance to the flow in the ends of the die. However, the larger manifold has some disadvantages, such as the longer residence time which leads to a stagnation of the flow nearly the ends of the die. At the same time, even if the augmentation of the manifold section leads to a resistance decrease, it is impossible to achieve an even flow since there will be always a pressure drops and by consequence, less flow at the ends of the die than at the centre.[64]

Variations in the thickness of the film can be caused by a non-constant flow over time, by a non-homogeneous fluid in terms of temperature and mixture or by some measurement errors in viscosity and even by theoretical flow calculations. A flexible lip is required to compensate these flow variations and to provide a fine adjustment. Therefore, the design of the lips is very important in the deposition performance.

13

To guarantee the quality of the slot die deposition process and for instance, the thin film thickness, there are more parameters to take into consideration than the manifold and lips design. The processing velocity, the flow rate given by the peristaltic pump and the distance between the substrate and the slot die, the angle between the fluid and the substrate (angle of the slot die) and the lips aperture are very important variables to control. The adjustment of these parameters is dependent on the characteristics of the coating/deposition material (viscosity) and the control of the deposition process is very dependent on the stability of the system and the operator experience [64].
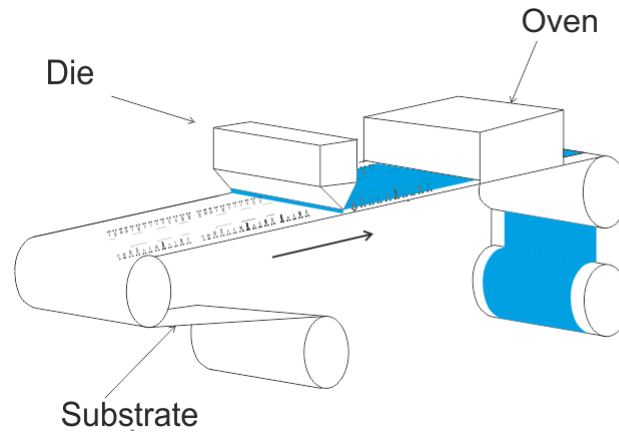
Figure 2.3-1 - Scheme of a R2R slot die printing system.

2.4. Two points probe method

Normally, PEDOT:PSS films are electrically characterized by the measurement of their sheet resistance. To measure the sheet resistance normally, either the two-points probe method or the four points probe method is used. In order to measure the sheet resistance, the thickness of the film needs to be approximated to zero which in practical terms, means that the sample's thickness needs to be considered negligible comparing to its width and length[65].

In this work, the two points probe method was used in order to characterize the PEDOT:PSS films. This method consists in two electrodes of exactly the same size placed parallel to each other and used in contact with the surface of the sample. Figure 2.4-1 schematically resumes the 2-point probe method.

Considering this method the sheet resistance can be calculated by **(2.4-1)**

$$R_S = \frac{V.W}{I_s.L},$$
(2.4-1)

where V is the applied potential, and I_s is the surface current measured in the films. In this work the method was applied for the same value of W and L so that the value of resistance was easily obtained. In this case a *Keitlhey 6487 picoammeter* was used both as voltage source and ammeter.
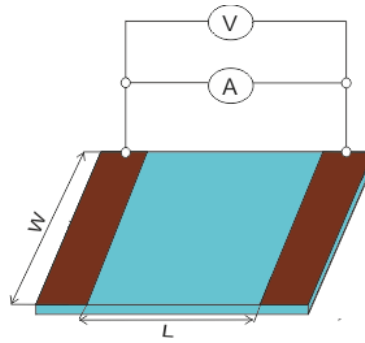
Figure 2.4-1 - Two point probe method scheme.

2.5. Analytes

The main goal of the present work is a development of an "electronic nose" for gynecological diseases detection. The choice of such area is of the enormous importance. The vagina contains a lot of small glands. The secretion of glands (different from the glands of the skin) covers area and forms a thin protective layer against urine, bacteria and menstrual blood. The vagina itself is an 8cm tube which extends from the vestibule to the cervix (opening of the uterus). On both sides of the cervix, vagina expands outwardly in a bag which is called the fornix. In these fornixes, especially at the rear, it can accumulate secretions from cervix and some cell debris. The vagina itself has no glands, but is lubricated by secretions from the cervix. Normal vaginal discharge has a pleasant smell, smooth and milky white cream or aspect of egg white, depending on the timing of the menstrual cycle. The vagina is covered by a protective and very strong mucosal tissue. The thickness of this tissue is determined by the balance of sex hormones. This balance changes during the menstrual cycle, during pregnancy and with age. As for young girls and older women, the mucosal tissue is only a few cell layers thick. Therefore, this tissue is very vulnerable and the balance of the vaginal environment can be easily disturbed. This is one of the main cause of gynecological diseases [66].

In the vagina (as well as for example in the mouth and intestines), a large number of microorganisms live in equilibrium with each other and with their host. This is called "vaginal flora". It is important to know that the vagina usually has an acidic environment (low pH). Some women will have heard of Lactobacillus vaginalis as useful bacteria. Lactobacilli - producing lactic acid bacteria – precisely, for its lactic acid production capacity. These bacteria largely determine the acidity of the vaginal environment. Notwithstanding, the same rule is also valid in this environment: the excess is detrimental. Among some women, we noted an excess of lactobacilli. When this is accompanied by complaints similar to those caused by candidiasis, normal diagnosis is 'candidiasis'. Usually, these women are treated for candidiasis and of course, without success. Along with lactobacilli (rod shaped bacteria), other bacteria are always present, for instance coconuts (rounded bacteria) belonging to the gut flora. They are certainly useful, but the presence of a number of these cocci is acceptable in a healthy vaginal environment (a mixed flora). When lactobacilli are absent, proper acidity of the vagina protection also disappears. In this case, the vaginal environment became alkaline (as opposed to acidic). This environment enhances the overgrowth of coccoid bacteria often resulting in infection called bacterial vaginosis. We can say that the natural protection of the vagina is determined by several factors; layers of cells of the vaginal mucosa, the vaginal acidity (pH), the balance between the microorganisms and the general state of health of a woman. The upset balance of the vagina has some consequences. In the worst situations, it can result in infection and inflammation. Disturbances may be caused by external and internal factors, or by a combination of both [66].

15

In this way, the premature and much more important, the correct determination of the typical kind of vaginal diseases became one of the most important area for health care as more than 50% of women suffer at least one gynecological problem during her life. A correct determination of the pathology leads to a correct treatment.

In this work, an analyte based on lactobacilli culture was used for testing purposes. The culture was added to a vaginal simulant [67] that reproduces the normal vaginal fluid conditions. The bacteria concentration is quite low (20% in volume) as an attempt to reproduce an early appearance of the Lactobacilli problem. Thereinafter, they are called as "infected – 20% of bacteria in vaginal simulant" and "normal – only vaginal simulant" respectively. The simulant has proved useful for research into contraceptive and prophylactic drug delivery and was developed to have the same physical and chemical properties known to influence intravaginal gel.

2.6.   Experimental Setup

The experimental setup, was firstly developed in an own concept of the main traditional systems used for the electronic nose analyte detection. In the Figure 2.6-1, a scheme of the experimental setup is shown. The idea is to force the air in the sample chamber to flow to the sensor chamber by opening the valve V1 and V2 and closing the valves V3. The sample chamber air can be then detected by the sensor. It was also built a system to control the environmental variables such as temperature, pressure and humidity which can influence the sensor response. The sensors are connected to the computer where all the data can be stored and analyzed (a microcontroller system connected by USB). The valve V3, is used to make a purge and clean the air inside the sensor chamber.

To measure the resistance values a *Voltage/Source Meter Keithley 2410* was used and in order to perform capacity measures an *RLC Meter Fluke PM6306* was used.
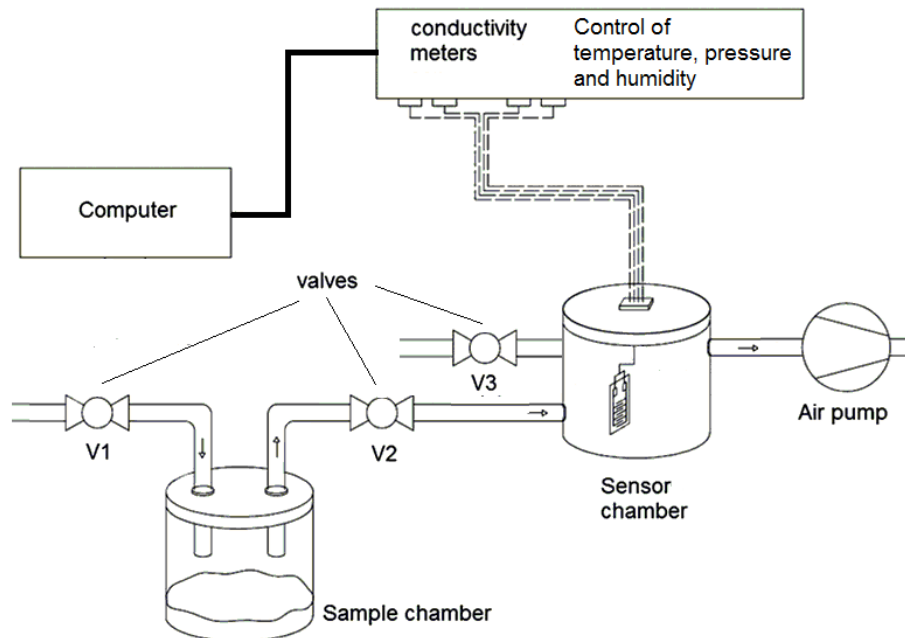
Figure 2.6-1 - Scheme of the experimental setup.

3. Materials and sensors' processing

3.1. Interdigitated Microelectrodes Design & Geometries

After a literature research about microelectrodes used in sensor technology, especially in gas sensors and odor biosensors, it was found that there is a gap of information about the influence of the geometrical parameters of the microelectrodes in the sensor's performance. Most of the works show that the use of interdigitated microelectrodes is preferred, instead of simply parallel electrodes, which is easily explained by the optimization of the active sensing area of the interdigitated electrodes (IMs) comparing to the parallel ones [58]. However, if we analyze the geometries of the IMs, it seems that the criteria of choice is almost empiric, since there is almost no specification about the shapes and dimensions of the microelectrodes.

Taking into consideration this gap of information about the geometrical parameters of microelectrodes and their influence in sensor performance, it was decided that this work was a good opportunity to study some of these parameters.

In order to accomplish this task, the first step was to identify and to define the geometrical parameters of an IM. Therefore, after analyzing the IM design, the following geometrical parameters were identified:

- Geometrical shape of the electrode: Rectangular, Rectangular with different corner shape, Circular, Hexagonal
- Electrode Area, A.
- Gap width, G.
- "Fingers" width, e.
- G:e ratio
- Electrodes width, l.
- Electrodes height, h.
- Number of "fingers", n (number of interdigitated pads)
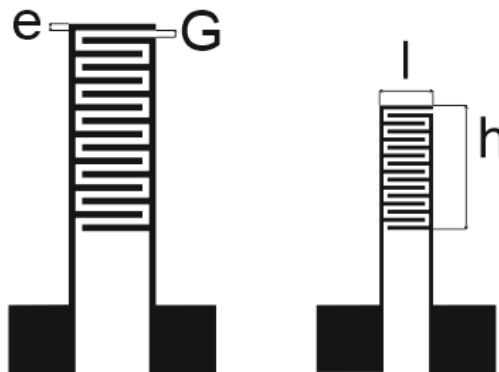
Figure 3.1-1 - Reference electrodes

In the previous work [58], 4 types of IM were studied. All of these electrodes had the same geometrical shape (rectangular) and the same number of "fingers" (n=16). Since the objective was to analyze the influence of the Gap and the fingers width, in order to keep the number of fingers constant, the electrodes had different areas according to their respective G and e. In all of these IM, the ratio of G and e, was kept constant and it was of 1:1. The electrodes which exhibited better performance were

the electrodes with G and e equal to 300 µm and 500 µm. These electrodes are exhibited in the Figure 3.1-1 and their geometrical parameters are shown in the Table 3.1-1.

Table 3.1-1 - Geometrical parameters of the reference electrodes

	Geometrical Shape	Area (mm²)	n	l (mm)	h (mm)	G (mm)	e (mm)	G:e	Abbrv.
IM$_{500}$	Rectangular	104= A$_{500}$	16	6.50	15.5	500	500	1	$^{20}\mathrm{IM}_{ref}{}^{1}{}_{500}$
IM$_{300}$	Rectangular	37.2= A$_{300}$	16	4.0	9.30	300	300	1	$^{20}\mathrm{IM}_{ref}{}^{1}{}_{300}$

For the current work, the objective was to understand better the effects of geometry variations in IMs, new electrodes were designed. Since in the previous work the area of the electrodes was not kept constant, it is difficult to compare directly the sensor response with G or e, since it is expected that the increase and the decrease of the electrodes area, affects the sensor response since the sensing areas are also being changed. Thus, following the results of the previous work it was decided to use as reference electrodes the IMs with G and e of 300 µm and 500 µm and to obtain variations of the geometrical parameters of both. For simplicity in this piece of art, the reference electrodes are IM$_{500}$ and IM$_{300}$, their areas A$_{500}$ and A$_{300}$, their width l$_{500}$ and l$_{300}$ and their height h$_{500}$ and h$_{300}$.

The first variation, affected the electrodes width (l) and height (h). The values are shown in the Table 3.1-2.

The variations of the parameters were divided in two groups with the objective to control separately the variables Area and number of fingers. Thus, in the first group the criteria, was to keep a constant A, equal to the reference electrodes, and to select the l and h variations which matched a specific variation of n (20 or 12). In the second group of these electrodes l and h were modified alternately while the area changed. The magnitude of the variations of l and h was the same as the one done in the first group in order to compare the effect of the variation of n with A.

The first group allows only the analysis of variations in the proportion between l and h, since both dimensions are varied at the same time. Therefore, with the second group it's possible to analyze separately the influence of the variation of both parameters. The consequence is an increase of the area of the electrodes.

The second geometrical parameter variation which was planned to analyze was the size of G and e, and the proportion between both. In order to accomplish this analyses, another two groups of electrodes were designed, both with the objective to vary G and e and simultaneously keep A constant. The geometrical parameters of the electrodes are shown in the Table 3.1-2.

In the first group of electrodes, A was kept constant, and width the same value of the reference electrodes while G and e were modified alternately. Once again, in this group of electrodes the modifications done in G and e values matched a specific n. In this case for the IM$_{500}$, the chosen n was again 20 and 12. For the IM$_{300}$, it was not possible to choose the same values since the dimensions of G or e would be too small for the printing resolution achieved with the screen printer available at our facilities. Thus for IM$_{300}$, it was chosen a smaller limit of variation of the parameter n, equal to 18.

In the second group of electrodes, n was kept constant and the objective was to analyze the effect of different $G:e$ ratios. The electrodes were designed to have a G more or less 60% bigger and 60 % smaller than the "e".

The last variation in the geometrical parameters of the rectangular IMs, was done in the shape of the fingers. Grover, William Henry et al, concludes in his work that the IM sensing area is affected by the shape of the corners of the fingers. In fact, G is not constant in all electrode since in the corners of the electrodes this parameter is increased by a $\sqrt{2}$ factor. The 90^0 angle formed by the corners doesn't allow to keep a constant G through all the electrode and hence the resistance increases with the distance between the electrodes and the capacitance is inversely affected by the same factor, the sensor sensitivity is affected in both resistive and capacitive modes. Even considering that this factor is probably too small to affect considerably the sensor performance, a new rectangular IM design, also proposed by Grover, William Henry et al [50], was developed. In this design, see *Figure 3.1-2*, the corners are erased and they are switched by a round shape which allows to keep the G through all the IM.
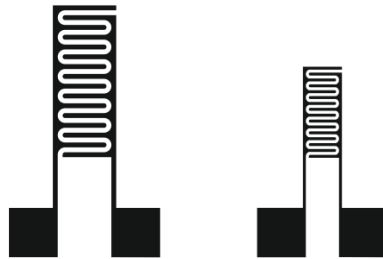
Figure 3.1-2 - New circular corner shaped electrodes
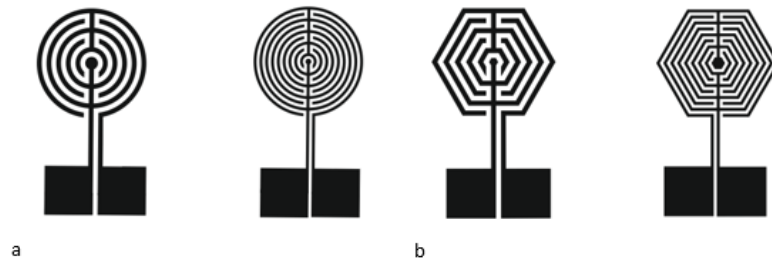
Figure 3.1-3 - Electrodes with different shapes: a) Circular. b) Hexagonal

New IMs with different geometrical shapes, circular and hexagonal, were also designed. It is expected that the change in the geometrical shape also changes the interface between the deposited conductive polymer and the electrodes which consequently alters the sensor response. Circular electrodes have already been used in some works especially in electrochemical sensors. Hexagonal shaped IMs are also proposed by Grover, William Henry et al [50], as a possible good alternative for the construction of arrays of sensors, since the hexagonal shape of the sensors allows to save space in the device.

These electrodes, shown in the *Figure 3.1-3*, were designed to have the same Area and G and e parameters of the reference electrodes IM_{500} and IM_{300}. The Table 3.1-2 shows all the geometric characteristics of the new microelectrodes designed in this work.

19

Table 3.1-2 - *Geometrical parameters of the new electrodes.*

	Geometrical Shape	Area (mm²)	n	l (mm)	h (mm)	G (mm)	e (mm)	G:e	Abbr*
IM dimension modification for a constant area	Rectangular	A_{500}	20	8.18	11.5	G_{500}	e_{500}	1	$^{20}R_{A500}^{1}$
			12	4.82	19.5				$^{12}R_{A500}^{1}$
		A_{300}	20	4.91	6.90	G_{300}	e_{300}		$^{20}R_{A300}^{1}$
			12	2.97	11.7				$^{12}R_{A300}^{1}$
IM dimension modification for a constant n	Rectangular	A_{500}	16	8.18	h_{500}	G_{500}	e_{500}	1	$^{16}R_{h500}^{1}$
				l_{500}	19.5				$^{16}R_{l500}^{1}$
		A_{300}	16	4.90	h_{300}	G_{300}	e_{300}		$^{16}R_{h300}^{1}$
				l_{300}	11.7				$^{16}R_{l300}$
Gap and pads' width variation for a constant Area	Rectangular	A_{500}	20	l_{500}	h_{500}	0.50	0.30	1.67	$^{20}R_{G500}^{1.7}$
			12			0.83	0.60	0.60	$^{12}R_{G500}^{0.6}$
			20			0.29	0.50	0.58	$^{20}R_{e500}^{0.6}$
			12			0.86		1.72	$^{12}R_{e500}^{1.7}$
	Rectangular	A_{300}	18	l_{300}	h_{300}	0.30	0.23	1.30	$^{20}R_{G300}^{1.3}$
			12				0.50	0.60	$^{12}R_{G300}^{0.6}$
			18			0.23	0.30	0.77	$^{20}R_{e300}^{0.8}$
			12			0.52		1.73	$^{12}R_{e300}^{1.7}$
G:e variation	Rectangular	A_{500}	16	l_{500}	h_{500}	0.29	0.70	0.41	$^{16}R_{A500}^{0.4}$
	Rectangular	A_{500}	16	l_{500}	h_{500}	0.72	0.29	2.50	$^{16}R_{A500}^{2.5}$
Different fingers' shape	Rectangular	A_{500}	16	l_{500}	h_{500}	G_{500}	e_{500}	1	$^{16}F_{n500}^{1}$
	Rectangular	A_{300}	16	l_{300}	h_{300}	G_{300}	e_{300}		$^{16}F_{n500}^{1}$
Different geometrical shapes	Circular	A_{500}	6	l_{500}	h_{500}	G_{500}	e_{500}	1	$^{6}C_{G500}^{1}$
	Circular	A_{300}	10	l_{300}	h_{300}	G_{300}	e_{300}		$^{10}C_{G300}^{1}$
	Hexagonal	A_{500}	6	l_{500}	h_{500}	G_{500}	e_{500}		$^{6}H_{G500}^{1}$
	Hexagonal	A_{300}	9	l_{300}	h_{300}	G_{300}	e_{300}		$^{9}H_{G300}^{1}$

*The notation abbreviations are completed and explained further in this work.

3.2. Screen Printing

The Screen Printing technique in this work was performed by a *Roku Print 2.2* screen printer [68] (Figure 3.2-1), on a flatbed disposition system..

Before the final printing process, a method to print the electrodes in order to let them prepared to be further processed by Slot Die, needed to be planed and prepared.

The Screen Printing Process is constituted for the following steps:

1) Spread the selectively blocking ink, in blue color, over the non-used areas of the mesh. This blue ink, blocks the columns of the mesh and allows the detailed defining of the printing area of the mesh.
2) Place the mesh in the Screen Printer support.
3) Calibrate the Setup: Mesh position, inclination, squeegee position.
4) Program the Scree Printer.
5) Place the substrate over the Screen Printer table.
6) Print.
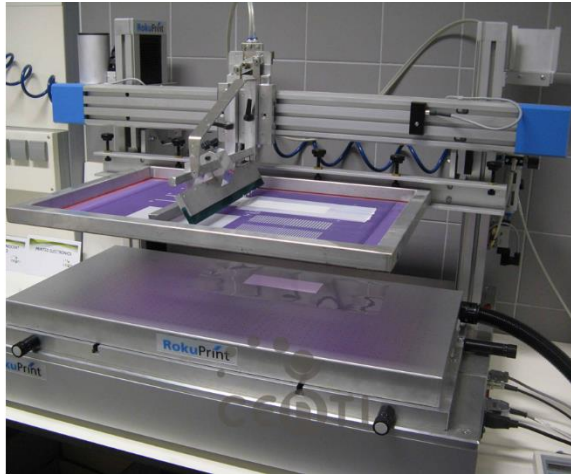
Figure 3.2-1: Roku Print 2.2 screen printing system used in this work.

To adjust the printing process in order to allow that during the slot die printing process the polymer is not printed over unwanted part of the microelectrodes, the roll and the mesh need to be calibrated and aligned precisely. Therefore in the 14 cm of width of PET the microelectrodes needed to be centered along the roll like it is shown further in the Figure 3.3-2

It was defined that every printing process was constituted by two different prints. The first print was done over the roll or PET in order to be possible to proceed to the slot die process after. The other print was done of a sheet of PET and the objective was to have an example control print of the process of every print done in the roll of PET.

First prints were made by using all the electrodes of the mesh, which corresponds to a large printing area, and means that all the electrodes were printed at the same time. However this process seemed to show bad results in terms of resolution and also on the wettability of the ink, which was difficult to maintain in these conditions. This lack of resolution into the printing of all the electrodes is related to the fact that the mesh due to the usage and aging has already a smooth inclination. This smooth inclination is the sufficient to allow the squeegee to do more force during a part of the mesh than the other. In consequence some electrodes seem have more resolution than the others and which in this case means that a part of the electrodes have a higher thickness than the other. Since the thickness of the electrodes has obvious consequences in the conductivity of the electrodes and the objective is to keep all the electrodes with the same characteristics, this process needed to be changed.

Therefore a new process was created where the initial printing area was divided in three parts. Consequently the MIs were printed in three parts and each part of the mesh was printed 6 times both in the Roll and in the PET sheets for control.

Optical Microscopy was made to some of the control sheets. To analyze the printing resolution but also the conductivity of the printed carbon pads, only the central parallel lines of the mesh were analyzed.
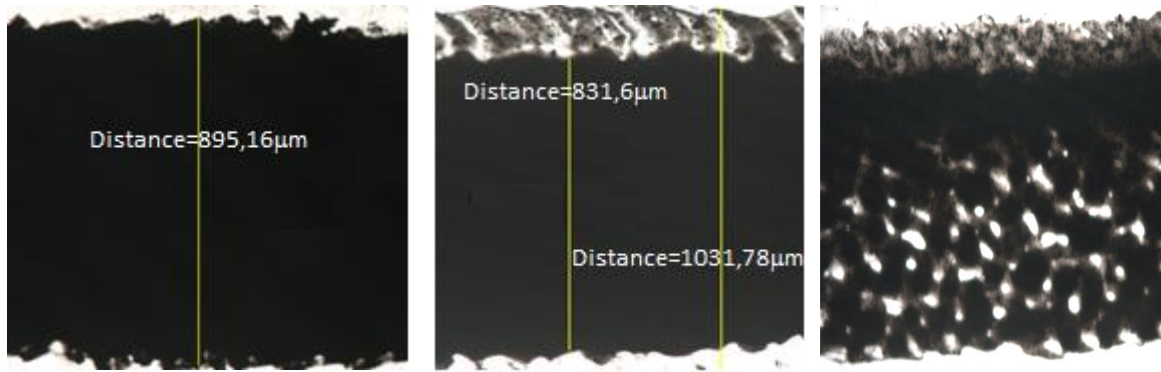
a)   b)   c)

Figure 3.2-2 - Optical Microscopy images obtained from the screen printed carbon microelectrodes. a) Best resolution. b) Good resolution with a border defect. c) Worst resolution.

As it can be seen form the results obtained by Optical Microscopy, the resolution the electrodes can vary significantly and there are some defects that can be found in the electrodes. Two of the most regular defects are shown in the Figure 3.2-2 b) and c). Good prints show a homogeneous printing but in some points the width of the pad is not the expected one. From both figures we can see that the boundaries of the pads have some irregularity. The Figure 3.2-2 a) shows a better resolution with a better defined boundary. In the Figure 3.2-2 c) we can see that in one of the sides of the pad the carbon paint spreads which affects the width of the carbon pad.

Defects such as the one shown in the Figure 3.2-2b), appears more often and it's normally due to a lower viscosity of the carbon paint. This happens because during the printing process the paint starts to dry and defects such as the one shown in the Figure 3.2-2c) start to be seen in the electrodes, and therefore to avoid it the mesh is cleaned carefully with the carbon paint solvent which turns the paint into a less viscous fluid.

A defect like the one shown the Figure 3.2-2b) is more regular and it seem to be intrinsic from a Screen Printing process like the one used in this work. Defects like the one found in the Figure 3.2-2b) affect considerably the conductivity of the electrodes and they are definitely to avoid. In order to prove that an analyses of resistance was performed in two different control pads of 2cm long. The resistance was measured by the two point probe method, and one of the samples showed good resolution like the one in a) and the other showed a bad resolution like the one in the Figure 3.2-2 c). 10 points of resistance were obtained between -1V and 1V with a step of 0,1V. For each electrode 10 resistance measures were performed in order to have an average and more reliable value of resistance. The results are shown in the Table 3.2-1.

Table 3.2-1 - Resistance values obtained from 2 cm long carbon pads.

	Resistance $(\Omega) \times 10^3$
Best Resolution	4,71
Worse Resolution	5,86

Later in this work will be explained that the electrodes obtained from this printing session were not tested as sensors.

Therefore in the ultimate printing session the process was improved in order to avoid major defects, showed in Figure 3.2-2(a, b and c). Naturally that the relatively high roughness of the carbon

electrodes surface as it can be seen by AFM (Figure 3.2-3), must imply that some electrodes areas could not be completely covered by PEDOT:PSS. Although such study was not done here, we expect that some electrical heterogeneities between electrodes must appear.
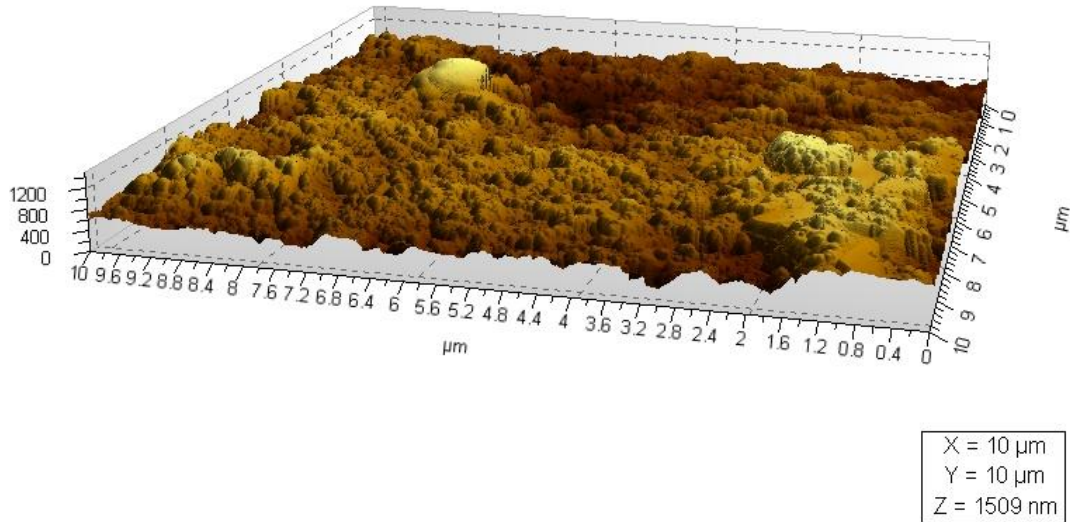
Figure 3.2-3: AFM analysis of the surface of a screen printed carbon pad.

In this printing session, the electrodes were only printed in two parts and not three. To avoid resolution defects the following method was executed:

1) After the first print in a PET sheet, check which electrodes have less resolution
2) Clean the mesh with the paint solvent with more intensity to the electrodes identified in the step 1) as the ones which have less resolution.
3) Print several times in normal paper till all the solvent is absorbed and the paint isn't too fluid.
4) Print 3 to 4 times in the roll and sensor control sheets
5) Repeat the last steps from the step 1) untill the end of the printing session.

By applying this effort it was guaranteed a better reproducibility and resolution of the microelectrodes.

3.3.   Slot Die

The slot die process is dependent on the polymer properties and on the selected solvent. The Figure 3.3-1 shows and image of the slot die printing system used in this work, a *Smartcoater* from *Coatema*. Different polymers solutions have different viscosities and so they will need different printing parameters. There are three main parameters that can be adjusted and an influence the deposition of the polymer solution: the distance from the lips of the head of the slot die system to the substrate, the flow rate of the solution in the pump and the velocity at which the substrate is moving. When varied this parameters influence the final thickness of the polymer. The closer the lips are from the substrate the tinnier is the final film of polymer. For the other parameters it seems also intuitive that the higher is the flow rate of the polymer the thicker is the film and inversely the higher the speed of the substrate the tinier is the film.

23
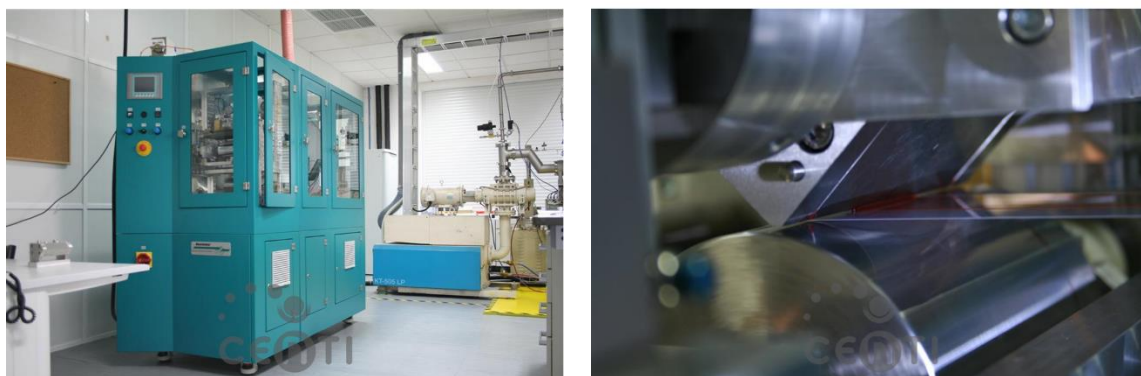
Figure 3.3-1: Smartcoater slot die printing system used in this work. a) The whole equipment; b) Image of a printing session.

Before any print in the roll with screen printed microelectrodes, the procedure was to print the grade of PEDOT:PSS in an clean roll of PET, varying the printing parameters in order to characterize the films and the influence of the variation of the parameters in their electrical and morphological characteristics.

It was grade of polymer was a PEDOT:PSS PH1000 from *Clevios*. This grade was also tested and used in previous work using the Spin Coating technique and it showed a response to analytes such as alcohol and acetone. However, during the process of characterization it was noticed that not only the films had a very high conductivity but they also hadn't any variation in the presence of the analytes. Therefore another grade of polymer needed to be used. The same procedure used with the other grade was repeated but, in this case, during the process it was clearly seen that the film showed a lot of problems of uniformity and resolution since the polymer was not aggregating to the surface of the substrate. It is known that for polymers such as PEDOT:PSS, surfactants such as $Triton^{TM}X$ can be added depending on the deposition/printing process. After exploring previous works and also state of art, it was decided to prepare three different solutions of 5ml of the grade of polymer with 0,1%, 0,2% and 0,3% of $Triton^{TM}X$. After several hours in a magnetic stirrer, each polymer was placed and spread in a sheet of substrate and it dried at the lab air temperature for half an hour. After the films were checked and it was decided that the solution with 0,2% of $Triton^{TM}X$ showed better uniformity and was the best to proceed to the slot die process.

Therefore, a solution PEDOT:PSS with 0,2% of $Triton^{TM}X$ was used in successfully, first over a clean roll of PET and after over the roll of PET with screen printed microelectrodes. The microelectrodes were printed taking in consideration of the possibility to print three different film thicknesses of PEDOT:PSS polymer over the microelectrodes. During the printing process, in order to vary the thickness of the film only the flow rate of the polymer in the pump was changed. The parameters which were used in the slot die process were the following:

- Distance of the lips to the substrate: 200µm.
- Roll speed: 0,8 cm.min⁻¹.
- Polymer's Flow rate: 1,7 ml.min⁻¹; 2,7 ml.min⁻¹; 3,7 ml.min⁻¹.
- Oven Temperature: 140 ºC.
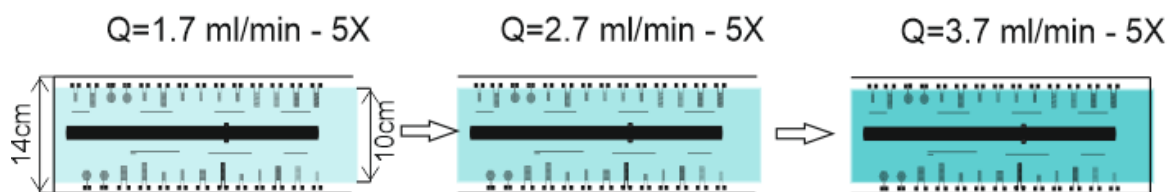
Figure 3.3-2 - Scheme of the slot die printing process used in this work.

The films of PEDOT:PSS were electrically characterized and their sheet resistivity was obtained using the two point probe method. For each value of flow rate, three different squared samples of 2cm were characterized and an average of the sheet resistance was calculated.

The thickness of the polymer was measured with an *AlphaStep D-100 KLA Tencor* profilometer. Three different measures were performed from three different parts of a film and the average value was calculated.

The Table 3.3-1, shows the values of the films sheet resistance for different values of polymer's flow rate and different values of thickness.

Table 3.3-1 - Correlation with the values of the flow rate used in the slot die printing process with the thickness and the sheet resistance of the obtained PEDOT:PSS films.

Flow rate (m.min⁻¹)	Thickness (nm)	Sheet Resistance ($\Omega.\square^{-1}$)
1,7	217,40	$1,05 \times 10^6$
2,7	315,22	$7,45 \times 10^5$
3,7	382,46	$5,98 \times 10^5$

After the fabrication of the sensors, Optical Microscopy (OM) was performed in order to evaluate the homogeneity of the PEDOT:PSS films. This analysis is difficult due to the fact that the films are very transparent and it's difficult to find the right contrast in the images to show the film. The images of OM are shown in the Figure 3.3-3.

Width values (µm)	478,85	486,90	479,78
Average value	481.84		
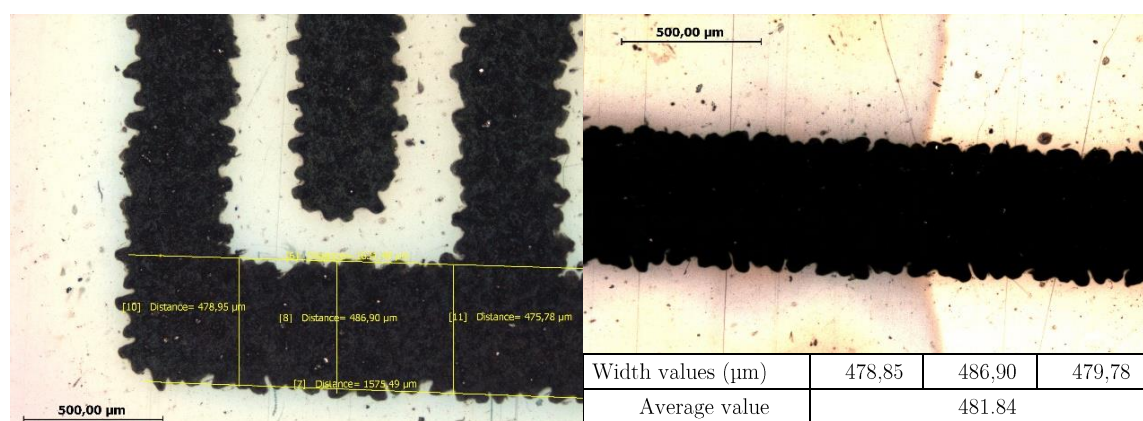
Figure 3.3-3 - Optical microscope images obtained from a sensor.

In these images obtained by OM it's possible to see that the microelectrodes have in general good resolution but still show some problems of resolution in the boarders. This affects only the width of the carbon pad that in this case it was expected to be 500 µm. It is very difficult to make a good analysis of the homogeneity of the PEDOT:PSS films, but it's also possible to see there aren't big irregularities and that near the boarders, the thickness of PEDOT:PSS is higher. What also can be

seen, is that in the boundaries between the polymer and the film, the line which defines this boundary is curved in the carbon pad. This little contraction of the line, is probably due to the fact that the polymer doesn't spread over the carbon pads as in the PET. However, in this case this aspect is completely irrelevant since it's not expected that this little irregularity will affect the behavior of the sensors. On the other hand, some roughness is expected on the top surface of the deposited electrodes. Such question can play an important role in the overall behavior, when a very thin film of polymer is deposited over that electrodes.

In this work, in order to facilitate the distinction between sensors with different parameters such as geometry, thickness and other parameters, a new nomenclature was created.

$$ {}_t^n X_{X_A}^{G:e} \, , $$

Where n, is the number of fingers of the microelectrode, $G:e$ is the proportion between the Gap width and the finger's width, t defines the thickness of the polymer's film which is described by the printing flow and finally A associates the microelectrode with one of the reference microelectrodes. For example, if a microelectrode is a variation of the geometrical parameters of the IM_{500} or the IM_{300} reference electrode, A will be equal to 500 or 300 respectively. Finally, X_X, is a character which is associated to the type of geometry or geometry variation of the microelectrode. For example, for a reference microelectrode C_G is $IM_{ref,}$ for the circular and hexagonal geometries it is C and H respectively. For the other microelectrodes the information can be seen in the Table 3.1-2, which summarizes all the information about the microelectrodes.

4.   Analysis and discussion of the results

4.1.   Introduction

After printing the sensors, and taking into account the big number of them available to test and the large number of variables which could be studied, it was definitely needed to define priorities and a plan of tests in which it would be possible to study and analyze the electrical response of the sensors. The obtained data and specific detailed information generated from the experimental setup was quite extensive, which due to all this aspect, it was necessary to create priorities in the analysis assessment.

From the departure, taking into consideration the fact that this was the first time that sensors of this type were printed with the combination of electronic printing technologies such as screen printing and slot die, and also with this grade of PEDOT:PSS (PH 1000), the main objective was to explore in a general way the behavior and the effectiveness of the resistive and capacitive electrical responses of the sensors when exposed to different analytes, especially the gynecological fluids simulators. Also, since three different thicknesses of conductive polymer were printed over the electrodes and since for the first time a large number of different geometrical parameters were varied in the electrode configurations, it was also a priority to evaluate the possible most prominent differences in the electrical responses from different geometries and thicknesses. Therefore, not all the geometrical parameters were tested but only those it was expected to exhibit distinctive behaviors.

During the tests the sensors were tested between the laboratory environment and the analyte environment. The sensors were tested first to the lab environment which served always as a baseline, and then to the analyte air. At least three cycles between laboratory environment and the analyte environment were performed. The cycles didn't have a precise duration but it was defined two minutes as a time reference. The temperature in the sensor chamber, during all the tests, didn't change significantly and was always between 23℃ and 24℃.

. Since the resistance values of the sensors, measured to the laboratory air, can vary from sensor to sensor, in order to evaluate correctly the response of the sensors the system, the results should be analyzed, not by the absolute value of resistance/capacitance measured during the test, but by their relative variance. In the current work, the results are generally discussed in terms of the relative variance of resistance/capacitance, which is calculated by $\left|\frac{\Delta R}{R_0}\right|$, in the case of resistance and by $\left|\frac{\Delta C}{C_0}\right|$. ΔR and ΔC are the difference the values of resistance/capacitance measured between the laboratory environment air (R_0 and C_0) and the air contaminated by the analyte.

In order to search for the limits of the sensors two tests where made with the objective to analyze the limits of the sensors when exposed to two kind of analytes: water and alcohol. These two analytes are present in many different analytes and it's known that organic polymer like PEDOT:PSS are very sensitive to these polymers.
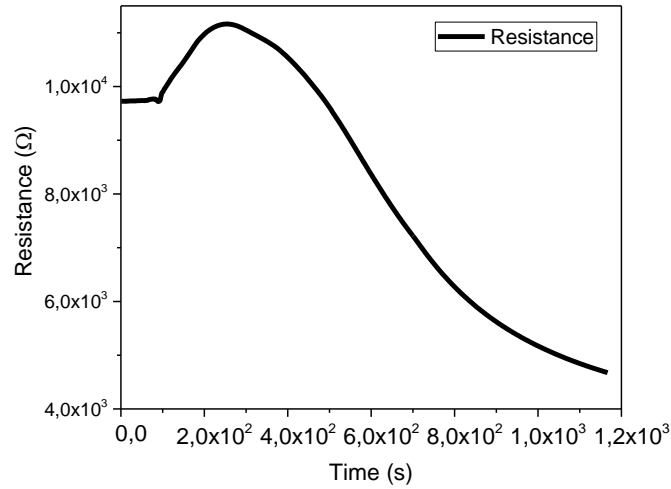
Figure 4.1-1- Resistive response of a sensor for the alcohol.

As it's possible to see in the *Figure 4.1-1*, the resistance when the sensors is exposed to the analytes the resistance first starts to increase. The resistance starts to stabilize at a certain point and then suddenly start to decrease. The resistance decreases considerably till a rupture point where the polymer stops to conduct any current.

This result also seems to confirm the behavior described by (4.1-1)[47].

$$\frac{1}{\sigma} = \frac{1}{\sigma_c} + \frac{1}{\sigma_h} + \frac{1}{\sigma_i},$$ *(4.1-1)*

where σ is the total conductivity, σ_c is defined as the intermolecular conductivity, σ_h is the conductivity due to hopping phenomena and σ_i is the ionic conductivity. In these results it seems that the conduction by hopping (σ_c), which is one of the dominant processes of electrical conductivity in doped PEDOT:PSS, starts to decrease. This happens because the polymer swells and the distance between PEDOT chains increase which difficult the hopping process. At some point, the overall conductivity starts to increase considerably and the resistance response describes a very well defined curve. This decrease of resistance can be explained by a sudden increase of the ionic conductivity of the polymer. Water and polar alcohols are good solvents of PEDOT:PSS and their absorption can start to dissolve surface of the polymer and a conductive ionic layer is formed on the surface of the polymer [69]. This increase of the ionic conductivity seems to be greater than the decrease of the hoping conductivity and the overall conductivity seems to increase until a point where the films possibly dissolve to a point where all the conductive paths are disrupted.

4.2.   Electrical characterization of the sensors

4.2.1. Reaction of different sensors of the same type to different analytes

At the beginning of tests, only resistance results were obtained. The tests were performed between the laboratory environment air and the normal vaginal fluid simulator environment. First tests had a pure exploratory objective, since it was needed a first notion of the type of resistive response of the sensors and especially to the gynecological analytes, in order to plan further tests.

28

Two different $_{3.7}^{20}\text{IM}_{ref}{}_{500}^{1}$ reference sensors were tested for the normal analyte and the infected analyte. At the beginning, one sensor of this type was tested to the normal analyte and then another one with the same characteristics was tested for the infected analyte
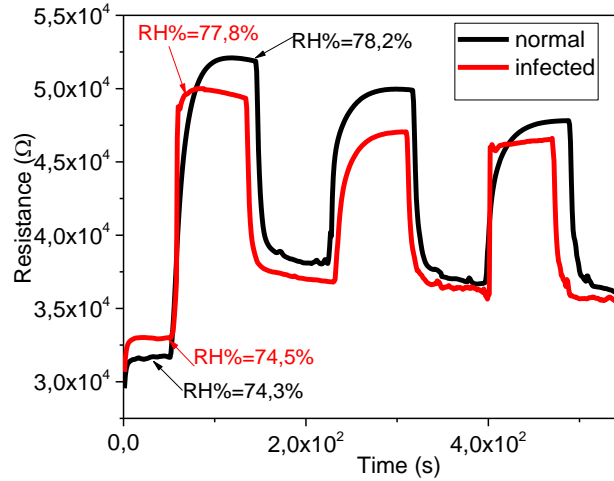
Figure 4.2-1 - Resistive response of different $_{3.7}^{20}IM_{ref}{}_{500}^{1}$ sensors for the gynecological analytes.

Table 4.2-1 - Values of the resistive response of different $_{3.7}^{20}IM_{ref}{}_{500}^{1}$ sensors for the gynecological analytes.

Test (Res)	Cycle	$\left\|\dfrac{\Delta R}{R_0}\right\|$
Normal	1	0,516
	2	0,276
	3	0,276
Infected	1	0,639
	2	0,308
	3	0,303

The results in the Figure 4.2-1 and in the Table 1.3-1, show that it's very difficult to differentiate the analytes with these two sensors. During this tests, it was also possible to observe that the sensors seem to react almost proportionally to the increase of the relative humidity (RH). It can also be seen that the "normal" analyte seems to increase slightly more the RH in the sensor chamber (78.2) than the "infected" analyte (77.8). Another remark, is that in the first cycle the sensor seems to react considerably more to the analyte than in the other two cycles. This behavior seems to show a non-reversible reaction between the sensor and the analyte.

Since the analytes are not very volatile and they have a big volume of water and since organic polymers are known to react considerably to the water and consequently to differences of humidity, it seemed possible that the sensors were reacting mostly to the molecules of water, and not to the analytes. Therefore, it was decided to perform a new group of tests. In this group of tests, three different sensors of a specific geometry and thickness were used to analyze three different analytes. It is important to clarify that each test was made with different sensors, but all of them had the same characteristics. For example, a $_{1.7}^{9}\text{H}_{G}{}_{300}^{1}$ sensor was used to analyze a water analyte, another $_{1.7}^{9}\text{H}_{G}{}_{300}^{1}$ sensor was used to analyze the normal analyte and another $_{1.7}^{9}\text{H}_{G}{}_{300}^{1}$ sensor was used to analyze the infected analyte. Apart

from the gynecological analytes, it was decided to analyze simply the water as an analyte. New geometries were chosen to be tested in order to understand, the influence of different electrode geometries in the resistive and capacitive behavior of the sensors. Sensors with the same thickness were tested in order to keep constant a variable that could change considerably the behavior of the sensors.

- $_{1.7}^{9}H_G{}_{300}^{1}$:
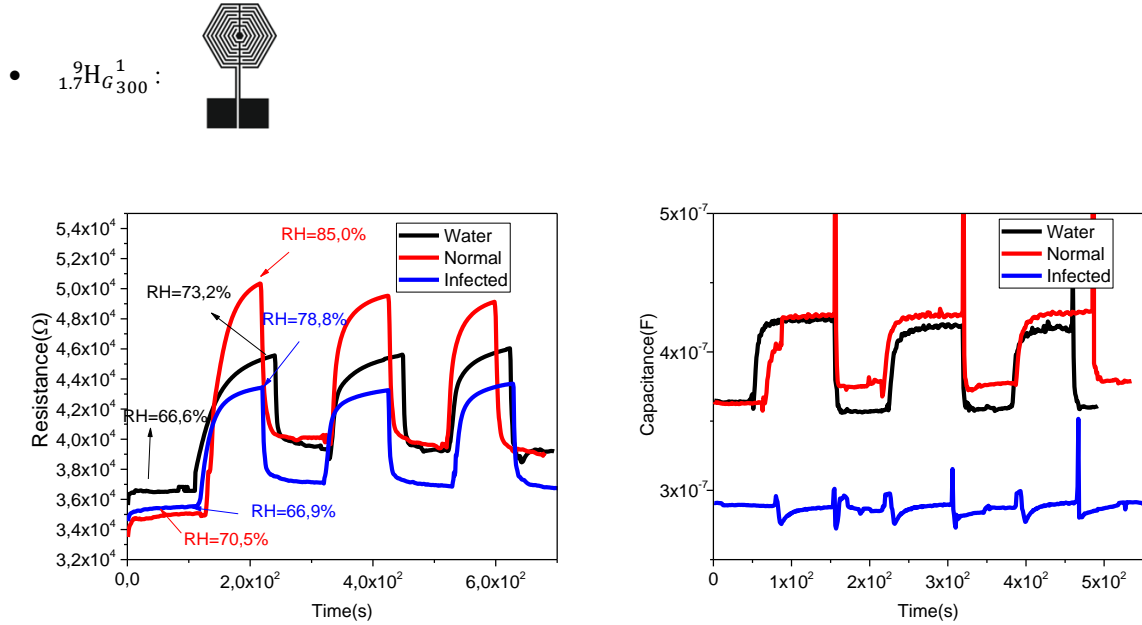
Figure 4.2-2 - Electrical response of different $_{1.7}^{9}H_G{}_{300}^{1}$ sensors to the analytes. a) Resistive response. b) Capacitive response.

- $_{1.7}^{6}H_G{}_{500}^{1}$
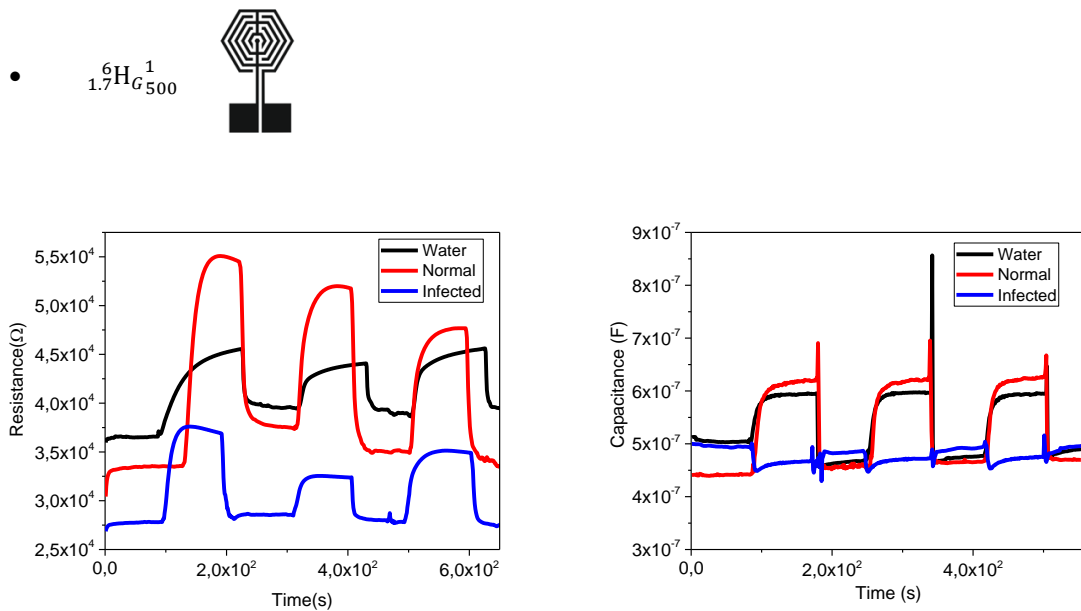
a)   b)

Figure 4.2-3 - Electrical response of different $_{1.7}^{6}H_G{}_{500}^{1}$ sensors to the analytes. a) Resistive response. b) Capacitive response.

- $^{10}_{1.7}C_G{}^1_{300}$

a)   b)

Figure 4.2-4 - Electrical response of different $^{10}_{1.7}C_G{}^1_{300}$ sensors to the analytes. a) Resistive response. b) Capacitive response.

- $^{6}_{1.7}C_G{}^1_{500}$

a)   b)

Figure 4.2-5 - Electrical response of different $^{6}_{1.7}C_G{}^1_{500}$ sensors to the analytes. a) Resistive response. b) Capacitive response.

Table 4.2-2 - Values of the electrical response of different sensors of the same type to the analytes.

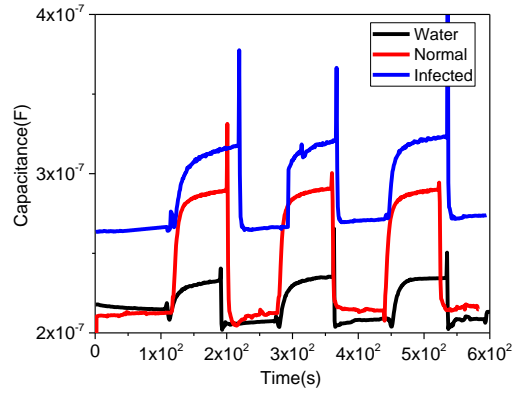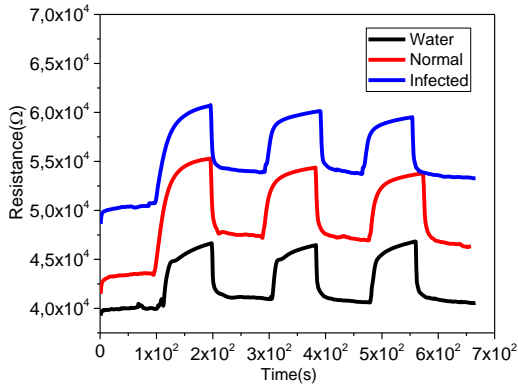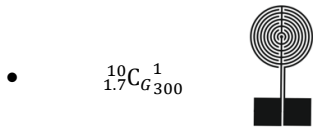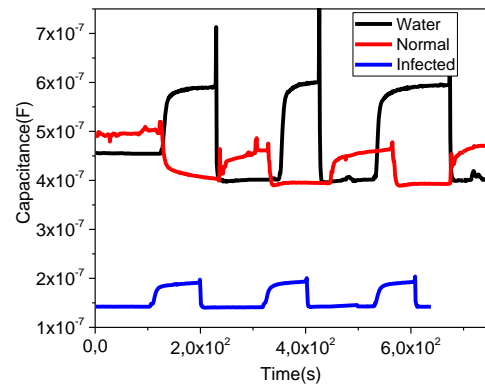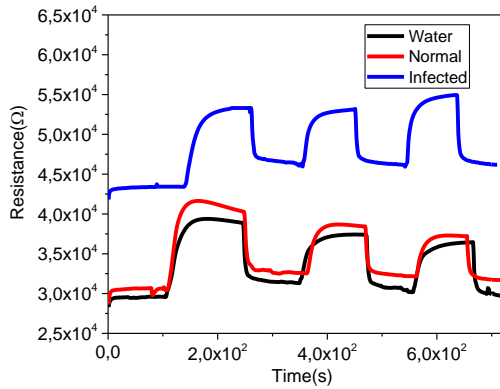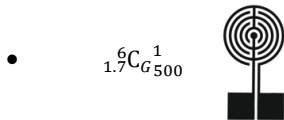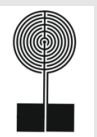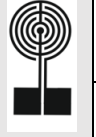| Sensor	Analyte	Cycle	$\left|\frac{\Delta R}{R_0}\right|$	$\left|\frac{\Delta C}{C_0}\right|$	Sensor	Analyte	Cycle	$\left|\frac{\Delta R}{R_0}\right|$	$\left|\frac{\Delta C}{C_0}\right|$
$^{9}_{1.7}H_{G\,300}^{1}$	H2O	1	0,248	0,175	$^{9}_{1.7}H_{G\,500}^{1}$	H2O	1	0,248	0,182
		2	0,176	0,135			2	0,169	0,182
		3	0,173	0,129			3	0,173	0,246
	Normal	1	0,441	0,164		Normal	1	0,644	0,401
		2	0,234	0,171			2	0,387	0,354
		3	0,242	0,162			3	0,361	0,342
	Infected	1	0,222	-		Infected	1	0,352	-
		2	0,165	-			2	0,138	-
		3	0,186	-			3	0,262	-
$^{10}_{1.7}C_{G\,300}^{1}$	H2O	1	0,167	0,083	$^{6}_{1.7}C_{G\,500}^{1}$	H2O	1	0,329	0,294
		2	0,133	0,134			2	0,191	0,495
		3	0,153	0,122			3	0,208	0,482
	Normal	1	0,269	0,362		Normal	1	0,360	0,194
		2	0,147	0,367			3	0,188	0,152
		3	0,145	0,354			3	0,158	0,160
	Infected	1	0,228	0,203		Infected	1	0,206	0,228
		2	0,149	0,201			2	0,113	0,150
		3	0,189	0,191			3	0,107	0,189

One of the first remarks from the analysis of the results shown in the Figure 4.2-2 4.2-3, 4.2-4 and 4.2-5 and resumed in the Table 4.2-2, is that the geometry of the IM has a considerable effect in the behavior of the sensors, especially in the capacitive mode. It's not surprising that the influence of the geometry is definitely higher in the capacitive mode, since the capacity is a physical variable which is dependent on the geometry of the conductor.

Another remark, and a crucial one, is that although the results in the resistive mode show different responses for different analytes, it seems that the differences are more due to the intrinsic variation between the responses of sensors with the same characteristics and also from the variation associated with the experimental setup, than from the general sensitivity of the sensors to the analytes. This can be concluded by the fact that, even between sensors of the same type there is a considerable difference of their baseline resistance. Another problem is that, again for each test the response can vary significantly from cycle to cycle, and even comparing the average of the three first peaks it's difficult to have values that can be possible to use in a future device to distinguish the analytes.

The capacity results show bigger variations of the sensors' response to the analytes. It is possible to see, in the case of both of hexagonal geometries, that the capacitive response to the infected analyte is completely different from the response to the other analytes, even if the response in resistance is similar between all analytes. Another interesting case is the response of the $^{6}_{1.7}C_{G\,500}^{1}$ sensor. In this case, the capacitive response is inverse comparing to the other analytes. However, even if this response is very interesting since it allows an easy differentiation to the analytes, it is important first to check if it's not an individual characteristic only of the sensor which was tested. Therefore, during the test the sensor was tested several times for the normal analyte and in the last two cycles for the water.
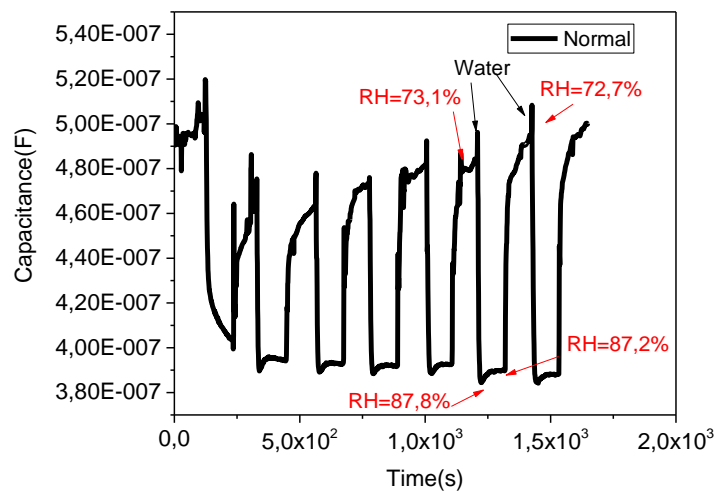
Figure 4.2-6 - Inverse capacitive response of a $_{1.7}^{6}CG_{500}^{1}$ sensor for the analytes.

As it can be seen from the graphic of the Figure 4.2-6, the response of the sensor had the same inverse behavior to the water, so it can be concluded that this type of response is characteristic only from this sensor. It must be noted that the analyte is composed mainly by water, as a basic solution of the vaginal simulant. Although such a question can appear as a problem, in fact, we are working in conditions that are expected in a real gynecology case. Another important remark is that in this case the sensor seems to have a higher response to the water comparing to the "normal" analyte. These different unexpected responses of the sensors with different geometries could be interesting if they would be reproducible. So far, after these results we are able to conclude that the effect of the microelectrode geometry can be considerable and if a reproducibility is achieved, maybe different geometries will permit better results in the differentiation of certain analytes. However, for these sensors with this grade of PEDOT:PSS and with this carbon ink, it's possible to conclude that the lack of reproducibility obtained by these complex geometries is not very promising, especially if we consider a possible standardized industrial development of sensors.

4.2.2. Reaction of a unique sensor to different analytes.

After the last group of tests, it was proven that it seems not to be possible to differentiate the analytes with different sensors of the same type. However, it is of obvious importance to understand if the PEDOT:PSS is or not, reacting differently to these analytes.

During first exploratory tests, as it can be seen in the figure below, it was possible to see that when the analyte is changed, from the normal vaginal analyte to the infected, during the same test, the sensor seems to have a smallest reaction to the infected analyte. This test was made with a $_{3.7}^{16}IM_{ref}{}_{500}^{1}$ sensor and the results are shown in the Figure 4.2-7 and in the Table 4.2-3.
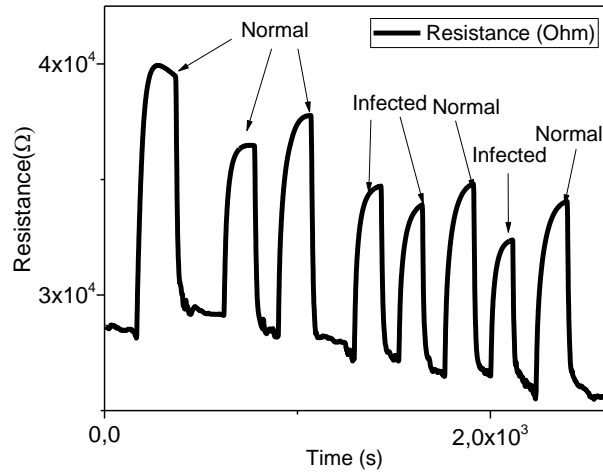
Figure 4.2-7 - Resistive response of a $_{3.7}^{20}IM_{ref}{}_{500}^{1}$ for both gynecological analytes during the same test.

Table 4.2-3 - Resistive response of $_{3.7}^{20}IM_{ref}{}_{500}^{1}$ to both gynecological analytes during the same test for both gynecological analytes, during the same test.

Analyte	Cycle	$\left|\dfrac{\Delta R}{R_0}\right|$
Normal	1	0,419
	2	0,252
	3	0,340
Infected	1	0,317
	2	0,320

Even if in the last test it seems that the sensor react in a different way with both analytes, it was not proved if a unique sensor can discriminate all analytes and prove that the polymer is reacting differently to all the different analytes.

Therefore one test was made with a $_{1.7}^{16}F_{n}{}_{500}^{1}$ sensor. This sensor was first tested twice to the water and only after to the analyte.

34
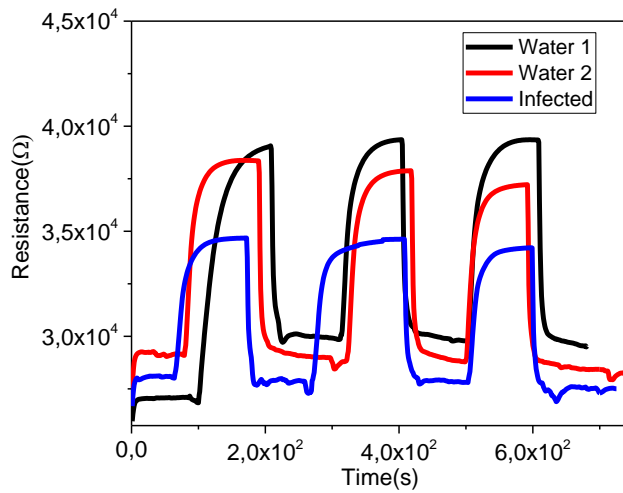
Figure 4.2-8 - Resistive response of a $^{16}_{1.7}F_n{}^1_{500}$ sensor in 3 different tests. 2 consecutive for water and 1 for the infected analyte.

Table 4.2-4 - Values of the resistive response of a $^{16}_{1.7}F_n{}^1_{500}$ sensor in 3 different tests. 2 consecutive for water and 1 for the infected analyte.

Analyte	Cycle	$\left\|\dfrac{\Delta R}{R_0}\right\|$
H2O - 1	1	0,439
	2	0,319
	3	0,321
H20 - 2	1	0,317
	2	0,320
	3	0,293
Infected	1	0,259
	2	0,242
	3	0,230

As it is possible to see in the results shown in the Figure 4.2-8 and in the Table 4.2-4, the same sensor seems to differentiate clearly the water and the infected analyte. The first two tests for the water seem to have the same response, and the last test for the infected analyte the sensor clearly shows a smaller response. This test, also proves that the sensor response to the same analyte, in this case the water, doesn't change between two consecutive tests.

After the last test, and in order to prove if it's possible to distinguish the analytes of the same type and at the same time prove that the polymer reacts differently to all the analytes, it was decided to use one unique sensor with a specific geometry and test it for the analytes with the following order: water-normal fluid-infected fluid. The same process was performed, using again different geometries in order to evaluate the influence of different geometries in the selectivity of one sensor.

- $^{10}_{1.7}C_{G}{}^{1}_{300}$
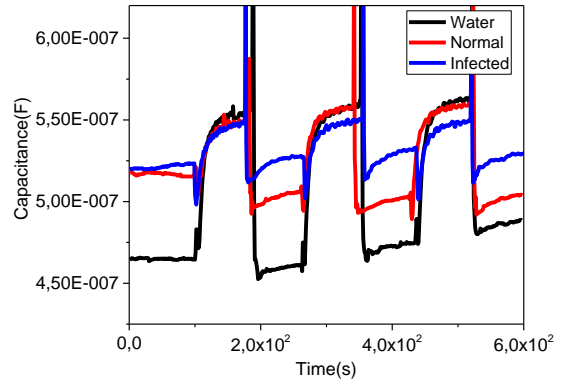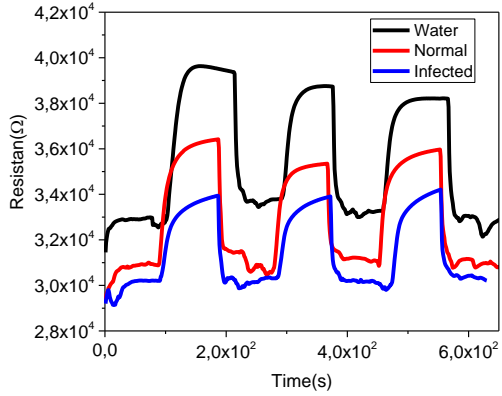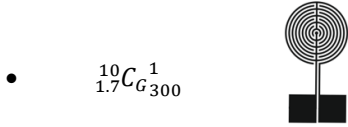
Figure 4.2-9 - Electrical response of a unique $^{10}_{1.7}C_{G}{}^{1}_{300}$ sensor for different analytes. a) Resistive response. b) Capacitive response.
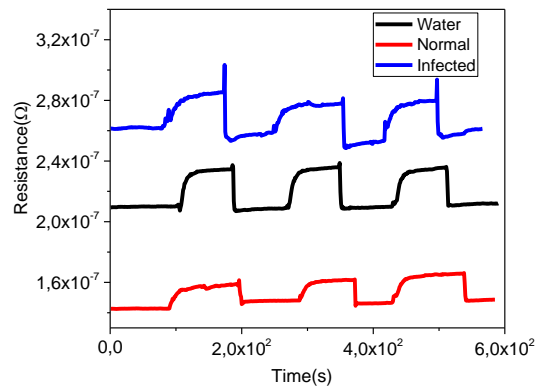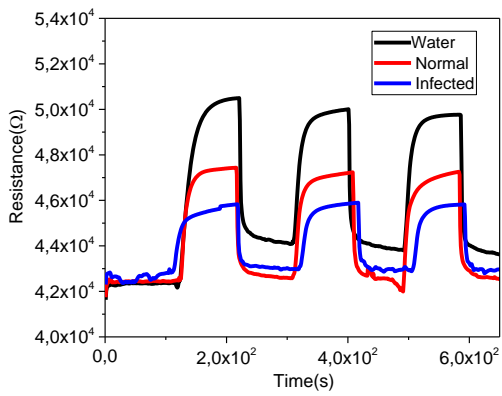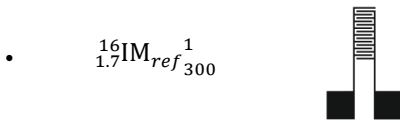
- $^{16}_{1.7}IM_{ref}{}^{1}_{300}$

a)   b)

Figure 4.2-10 - Electrical response of a unique $^{16}_{1.7}IM_{ref}{}^{1}_{300}$ sensor for different analytes. a) Resistive response. b) Capacitive response.
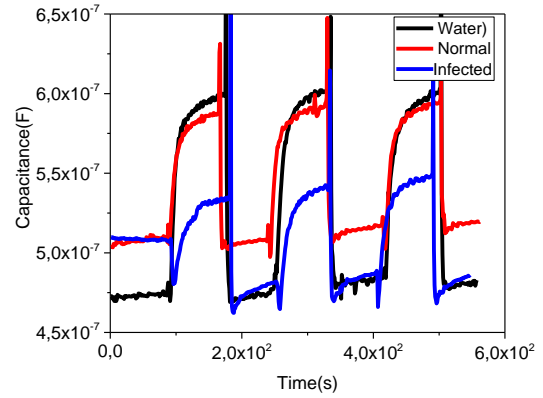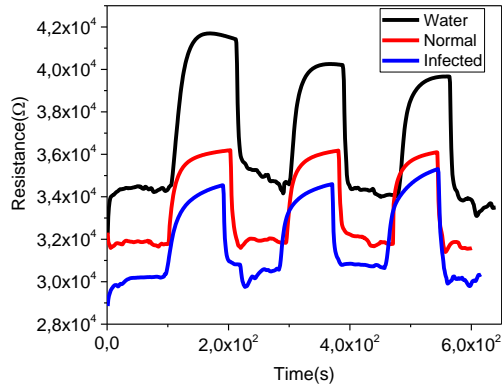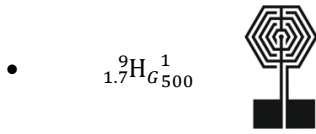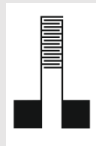
- $_{1.7}^{9}\text{H}_{G\,500}^{1}$

a)   b)

Figure 4.2-11 - Electrical response of a unique $_{1.7}^{6}H_{G\,500}^{1}$ sensor for different analytes. a) Resistive response. b) Capacitive response.
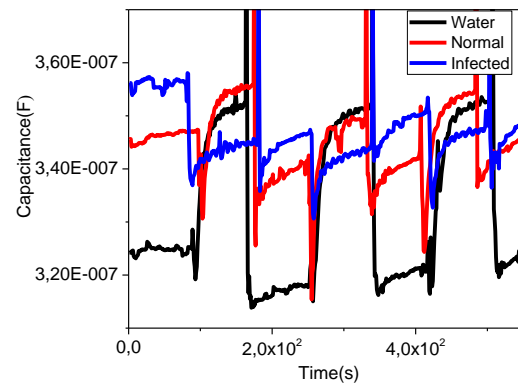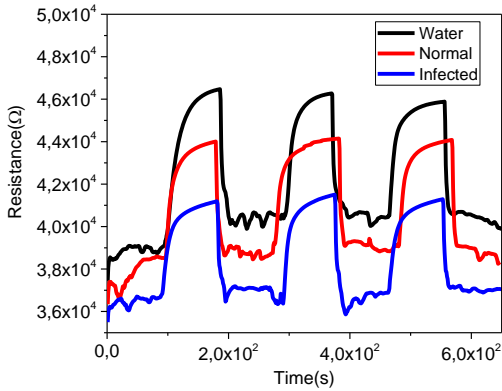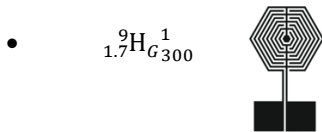
- $_{1.7}^{9}\text{H}_{G\,300}^{1}$

a)   b)

Figure 4.2-12 - Electrical response of a unique $_{1.7}^{9}H_{G\,300}^{1}$ sensor for different analytes. a) Resistive response. b) Capacitive response.

Table 4.2-5 - Values of the electrical response of a unique sensor for the analytes.

Sensor	Analyte	Cycle	$\left|\frac{\Delta R}{R_0}\right|$	$\left|\frac{\Delta C}{C_0}\right|$	Sensor	Analyte	Cycle	$\left|\frac{\Delta R}{R_0}\right|$	$\left|\frac{\Delta C}{C_0}\right|$
$^{10}_{1.7}C_{G\,300}^{\,1}$	H2O	1	0,214	0,195	$^{16}_{1.7}IM_{ref\,300}^{\,1}$	H2O	1	0,195	0,117
		2	0,147	0,213			2	0,134	0,131
		3	0,150	0,185			3	0,135	0,122
	Normal	1	0,179	0,063		Normal	1	0,118	0,113
		2	0,157	0,102			2	0,108	0,092
		3	0,158	0,114			3	0,120	0,130
	Infected	1	0,222	-		Infected	1	0,071	0,091
		2	0,165	-			2	0,068	0,078
		3	0,186	-			3	0,067	0,108
$^{6}_{1.7}H_{G\,500}^{\,1}$	H2O	1	0,217	0,263	$^{9}_{1.7}H_{G\,300}^{\,1}$	H2O	1	0,196	0,082
		2	0,162	0,273			2	0,144	0,107
		3	0,165	0,240			3	0,134	0,099
	Normal	1	0,139	0,151		Normal	1	0,141	0,024
		2	0,136	0,161			3	0,143	0,025
		3	0,139	0,150			3	0,126	0,036
	Infected	1	0,144	0,050		Infected	1	0,124	-
		2	0,134	0,124			2	0,133	-
		3	0,150	0,125			3	0,118	-

As it can be seen from the results of the Figure 4.2-9, 4.2-10, 4.2-11 and 4.2-12, and the values of the results resumed in the Table 4.2-5, the sensors seem to have different responses for the analytes. Even if these differences are very sharp, it seems that there is a pattern which show that the sensors reaction is higher for the water than the gynecological analytes in the resistive and in the capacitive mode. Then, when we compare the responses of the sensors to the gynecological analytes, it's possible to verify that the sensors have a higher reaction for the normal analyte, than for the infected analyte. Therefore, this pattern of results show that the sensors reaction is proportional to the quantity of water which is present in the analyte. Again, the results show that these type of sensors are very sensitive to the water.

It is important to note, that again the capacitive response of the sensors with complex geometries have a different and a less stable response to the analytes than the sensors with a normal rectangular geometry. As it can be seen in the Figure 4.2-9, Figure 4.2-11Figure 4.2-12, the response of these sensors to the water is more stable than for the gynecological analytes. In fact, when we compare also the capacitive responses to the "normal" and to the "infected" analytes it's possible to distinguish easily the analytes. The results show that the dynamic of response of the sensors for all the analytes is clearly different which can help easily to distinguish all the analytes.

Another interesting result, is the capacitive response of the $_{1.7}^{9}\mathrm{H}_{G}{}_{300}^{1}$ sensor. As it can be seen in the Figure 4.2-12 b), the response for the "infected" analyte is very unstable and completely different for the other analytes. This kind of result was also observed for these type of sensor in a previous result (see Figure 4.2-3 b)). Even considering the fact that the capacitive results show a considerable instability associated to the experimental setup, since for the same type of sensor and for the same analyte the responses are similar, it seems that this kind of response to the infected analyte is typical for this type of sensor. However, it is very important to refer that in order to conclude that a $_{1.7}^{9}\mathrm{H}_{G}{}_{300}^{1}$ sensor has this type of response new tests need to be made with more stable experimental setup for capacitive measures.

These results show that it's possible to differentiate the analytes However, this differentiation is only achieved using the same sensor to test all the analytes. For the desired application of these sensors it is necessary to ensure that the differentiation of the gynecological analytes can be done by different sensors which is still not the case.

4.2.3. Influence of the thickness of the polymer in the sensors response

Although it was already possible to see that the geometry of the electrode influences the electrical response of the sensor and especially the capacitive behavior, it was important in such a preliminary work to understand the importance of the thickness of the polymer film in the sensor response.

Two type of sensors of the same geometry, $^{16}\mathrm{IM}_{ref}{}_{300}^{1}$ and $^{16}\mathrm{IM}_{ref}{}_{300}^{1}$, but with different thicknesses of the polymer layer were tested for the infected analyte.
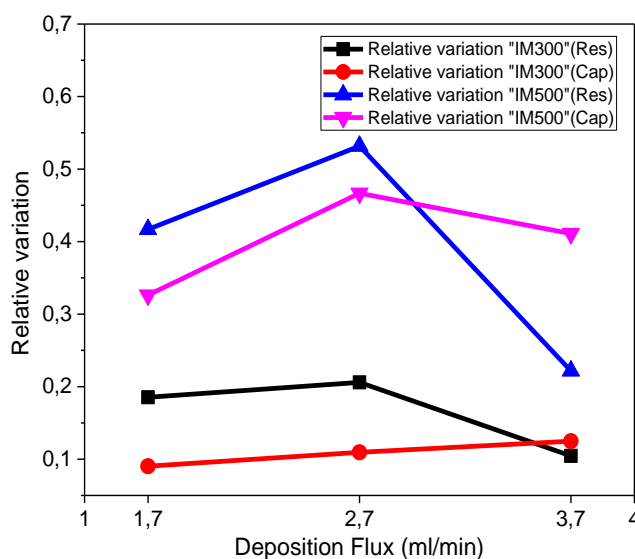
Figure 4.2-13 - Influence of the polymer thickness in the sensor electrical response for the "infected" analyte.

Table 4.2-6 - Values of the response of sensors with the same geometry, but with different thicknesses for the infected analyte.

Sensor	Flow rate (ml/min)	Cycle	$\left\|\dfrac{\Delta R}{R_0}\right\|$	Average value	$\left\|\dfrac{\Delta C}{C_0}\right\|$	Average value
$^{16}\mathrm{IM}_{ref\,300}^{1}$	1,7	1	0,181		0,065	
		2	0,195	0,185	0,085	0,090
		3	0,181		0,388	
	2,7	1	0,191		0,077	
		2	0,211	0,206	0,131	0,120
		3	0,217		0,120	
	3,7	1	0,0833		0,129	
		2	0,115	0,105	0,118	0,125
		3	0,116		0,126	
$^{16}\mathrm{IM}_{ref\,500}^{1}$	1,7	1	0,316		0,411	
		2	0,176	0,222	0,429	0,409
		3	0,173		0,388	
	2.7	1	0,878		0,498	
		2	0,357	0,531	0,435	0,467
		3	0,360		0,467	
	3.7	1	0,639		0,261	
		2	0,308	0,417	0,306	0,284
		3	0,303		0,289	

As it's possible to see in the Figure 4.3-13 and in the Table 4.2-6 the response of the sensors is dependent on the thickness of the polymer film. Although there is a dependence between the amplitude of the sensors response with their thickness, this dependence doesn't seem to be linear. In the resistive mode, there is a big difference between sensors with maximum thicknesses and the others. "3,7" sensors (sensors produced with a flow rate of 3,7 ml/min during the slot die process), have a smaller response than the "2,7" and "1,7" sensors, which have a higher and approximately similar response. In the case of the capacitive mode, sensors show the inverse relation with the thickness. In this case, there is a considerable difference between the thinnest sensor and the others. Then again between the "2,7" and "3,7" sensors the difference of the response seems to be irrelevant. In this case the amplitude of the response is also inverse when compared with the resistive mode, since it's higher for the highest thickness.

In this case it's possible to conclude that the polymer thickness which shows the best response is the middle one which corresponds to the "2,7" sensors, since in both modes, the resistive and the capacitive, it shows the best response.

4.2.4. Influence of different geometrical parameters in the sensors response.

During this work, as part of the scaling process for the production of this sensors, not only electrodes with different geometries were designed but also electrodes with the reference rectangular interdigitated geometry but with different dimensions and consequently proportions of G and e. In

order to realize if there is in fact a considerable difference in the response of these sensors varying these parameters $^{16}_{2,7}R_{G\,300}^{1}$ sensors were tested for the infected analyte.
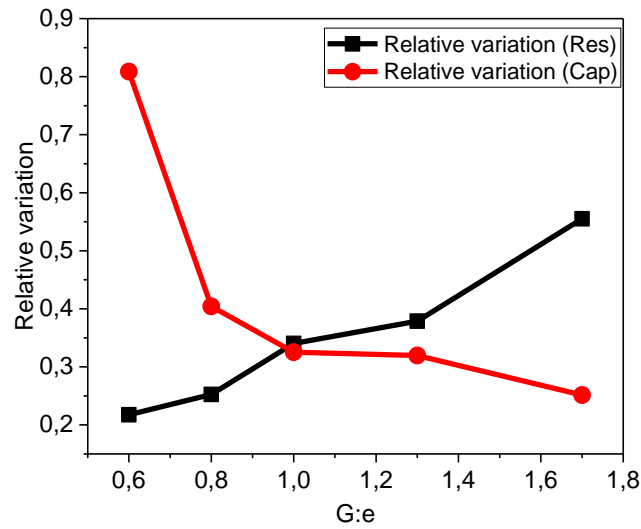
Figure 4.2-14 - Influence of the G:e proportion in the sensors response.:

Table 4.2-7 - Values of the electrical response of sensors with different G:e proportion, for the infected analyte.

IM	Cycle	$\left|\dfrac{\Delta R}{R_0}\right|$	Average value	$\left|\dfrac{\Delta R}{R_0}\right|$	Average value
$^{16}_{2,7}R_{G\,300}^{1}$	1	0,396	0,344	0,277	0,325
	2	0,346		0,347	
	3	0,279		0,351	
$^{12}_{2,7}R_{l\,300}^{1}$	1	0,385	0,293	0,343	0,369
	2	0,265		0,433	
	3	0,244		0,332	
$^{12}_{2,7}R_{h\,300}^{1}$	1	0,332	0,275	0,210	0,272
	2	0,253		0,302	
	3	0,241		0,308	
$^{20}_{2.7}R_{G\,300}^{1,7}$	1	0,220	0,555	0,814	0,251
	2	0,227		0,839	
	3	0,205		0,773	
$^{20}_{2.7}R_{G\,300}^{0,8}$	1	0,309	0,252	0,418	0,403
	2	0,233		0,428	
	3	0,215		0,367	
$^{20}_{2.7}R_{e\,300}^{0,6}$	1	0,737	0,252	0,231	0,809
	2	0,477		0,275	
	3	0,451		0,249	
$^{1.3}_{2.7}R_{e\,300}^{1.3}$	1	0,331	0,379	2,93	0,320
	2	0,413		3,34	
	3	0,393		3,31	

As it is possible to see in the results, there is a clear influence in some geometrical parameters in the resistive and capacitive response of the sensors. Geometrical parameters such as the width and the length of the electrodes, doesn't seem to have a considerable effect in the behavior of the sensors. However the variance of the size of the Gap or the width of the fingers has clear consequences on the resistive and capacitive response of the sensor. This result can be, in a first approximation, ascribed to the different electrical filed lines between the electrodes that are created at the polymer film, depending on the way that the polymer chains are oriented (specifically due to a local conformation of the molecules) with a strong influence on the electrical properties. Such dependence must be obviously related with the variance of the Gap size (change in the film area under electrical filed) as well the fingers width (much more conductive in this case). As it can be seen from the values in the

Table 4.2-7, it seems that the proportion between G and e influences the behavior of the sensors. According to these results, for the resistive mode the higher is the proportion G:e the higher is the response of the sensors. From the other side and even if only two proportion were tested it seems that the opposite relation takes place. In this case, the lower the proportion G:e, the higher the capacitive response. In the case of the lower G:e tested ($_{2.7}^{20}\text{R}_{e\,300}^{0.6}$),it can be easily considered by far which this geometry presents the best performance of all sensors tested, both in the amplitude of the response and the stability.

4.2.5. Analysis of the sensors response for different analytes.

Another important factor that can also contribute for the differentiation of different analytes with these sensors, is the fact that their response to some analytes can not only be different considering the amplitude of the response but also the response as a difference behavior which is translated in peaks with different forms almost as an analyte signature. The Figure 4.2-15 shows the reaction of a $_{1.7}^{16}\text{IM}_{ref\,500}^{1}$ sensor to different analytes alternately.
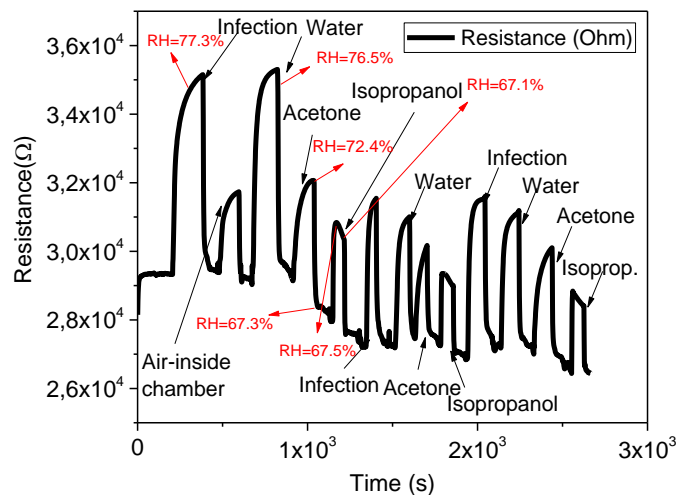
Figure 4.2-15 - Resistive response for different analytes during a single test.

This test shows that even if it is difficult to distinguish the responses of the gynecological analytes and the water, it is proven that for other analytes such as isopropanol and acetone, the sensor has a completely different response. As it possible to see, the responses of the sensors for isopropanol and acetone are singular and graphically it's possible to distinguish them directly from the shape of the resistance/time curve. This characteristic response is especially easy to see in the isopropanol curve and can be evaluated also through the derivate of the response, as it is shown in the Figure 4.2-16.

It can also be seen again the influence of the RH in the behavior of the responses. The responses for the infected analyte and for the water have a similar response in amplitude and in dynamic and the RH reaches also the same values in both cases (77.3% and 76.5%, respectively). But in the case of the acetone, even if the dynamic of the response is quite similar for the "infected" analyte and for the water, the amplitude of the response is considerably smaller and the RH reaches also a smaller value (72.4%).In the case of the isopropanol response, it is possible to see that the sensor reacts completely differently and much faster than for the other analytes. The increase of RH for the isopropanol is very small and it seems that in this case the sensor doesn't react to the water molecules, however after a first peak of resistance increase with a tiny increase of RH (67.3% to 67.5%) there is a smooth decrease of resistance, which is simultaneously followed by a decrease of RH to a value of 67,1%. Therefore, it's possible to conclude that acetone response, seems to be mainly influenced by the increase oh RH, but the resistance curve shows also already some differences in its shape comparing for the water and the infected analyte. The reaction for the isopropanol, shows that in the presence of this compound the RH doesn't play the main role on the sensor's resistive behavior, even if it seems there is a relationship of the sensor response with the drying role that the isopropanol seems to play in the sensor chamber.
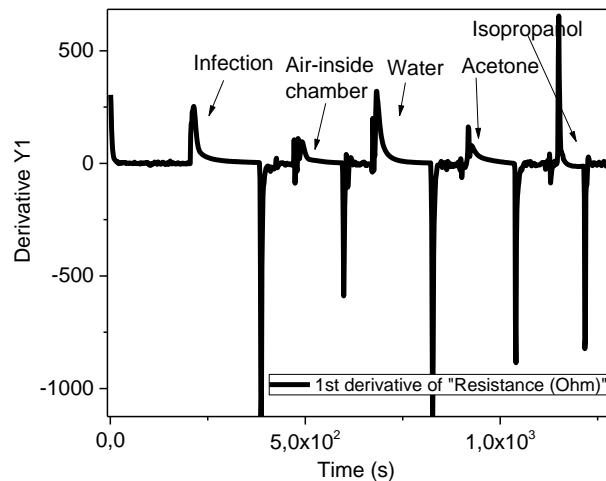
Figure 4.2-16 - First derivative of the resistance response curve.

Through the analysis of the first derivate curve, it is possible to see that it is easy to identify the isopropanol response from the others. In this case, the acetone response it's not so trivial to identify, however the amplitude of the peaks of acetone are smaller and the derivate response after the first peak relaxes slightly slower than in the case of the infected analyte and the water. For these last two analytes the difference between their responses is still very small and not regular enough to say that there is a possibility identify the analytes only by the analysis from one sensor.

4.2.6. Detection of blue cheese spoilage.

In the previous work [58], it was studied the response of these sensors to a fungal gynecological pathogenic analyte. In this work, other analytes were tested without a fungal origin. In order to test the possible reaction of these sensors to an analyte with a fungal origin the sensors were tested to blue cheese. This type of cheese is known for having a strong smell especially due to the fungal presence of the Penicillium family [70].

Therefore a $^{12}_{1,7}R_{l^1_{300}}$ sensor was tested to the presence of a blue cheese. Two types of blue cheese analytes were created. One of the samples was a small piece cheese kept in the fridge during one night

and the other was a piece of cheese kept outside the fridge at the normal environment temperature. The samples were placed in the test chamber as it was made with the other analytes.
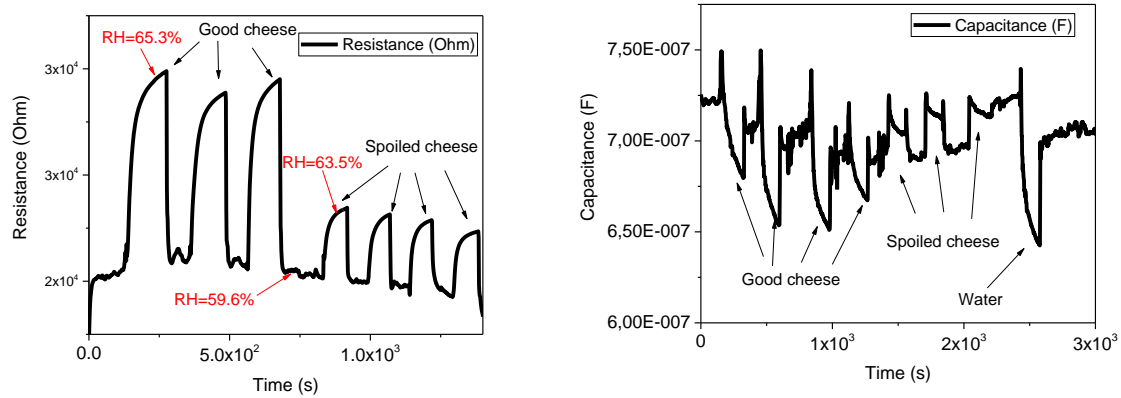
a)   b)

Figure 4.2-17 - Electrical response of a $^{12}_{2,7}Rl^1_{300}$ sensor for a good and a spoiled cheese. a) Resistive response; b) capacitive response.

These tests show that these type of sensors can clearly detect the presence of the cheese and they can also detect the spoilage of the cheese in the resistive and capacitive modes. In the Figure 4.2-17 a) it can be been seen that the sensor reacts with more intensity for the good cheese than for the spoiled cheese. This means that the increment of fungal specimens' volume seem to block the response of the sensor. However, again it the presence of water molecules is an important factor for the response of this sensors and the discrimination between analytes since the spoiled cheese is also drier than the good one as the RH values during the good cheese test were superior than the values obtained with the spoiled cheese. From the analysis of the capacitive response, in the Figure 4.2-17 b), an easy differentiation between the good and the spoiled cheese is also achieved. In this case, the capacity seems to decrease in the presence of the cheese. In this case, the capacitance decreases less in the presence of the spoiled cheese than in the presence of the good cheese.

The capacitance in the presence of the cheese decreases, which is a different result than what seems to happen for the other analytes. But in the presence of water it seems to decrease also in this test. The sensor which was used doesn't have a complex geometry, so its capacitance was expected to increase with the water as it happened in the previous tests.

44

5.   Conclusion

Since this project had a big technical basis the evaluation of the results relied not only in the sensors' characterization but also in the evaluation of all the methodology used in the fabrication of the sensors.

In this work, a new methodology for the development of microelectrodes for sensor purposes was used with success. The slot die printing process, proved to be a good technique for the scaling up process and for a future mass development of conductive polymer based gas sensors. Although an exhaustive optimization process still needs to be done, the results obtained in this work were positive especially when taking into consideration the future potential of this sensors. The good reproducibility achieved with these sensors shows that the screen printing process and the slot die process show good homogeneity and are definitely a viable solution to the fabrication of these type of sensors.

Nevertheless, it is important to highlight that the difficulty to standardize, the screen printing process during this work is due to the fact that the screen printing device which was used, has a lot of manual mechanisms and depends considerably of the experience of the operator and many other factors that can vary between different printing sessions, such as different materials and even the different designs of the microelectrodes. However, in the future, for effective mass production of these microelectrodes, it's available in CeNTI facilities an equipment of roll-to-roll processing of flexible thin-film devices (*MicroFLEX from 3D MicroMac* [71]) which is a device prepared for mass production of these devices and which will increase considerably the reproducibility and consequently the viability of the screen printing and also the slot die processes.

As far as the characterization is concerned, the first and the most important conclusion to be drawn, especially considering the objectives defined for this work, it is the fact that the sensors showed sensitivity and a stable response to different analytes.

However, in comparison to the results obtained in the previous work, with sensors processed by spin coating and with a different grade of PEDOT:PSS (PEDOT:PSS PH500 commercialized by Clevios™), the results showed that the new sensors are considerably less sensitive. This decrease of sensitivity obtained with the new sensors, it's related mostly with the different grade of PEDOT:PSS used in the current work. PH 500 is a more resistive grade of PEDOT:PSS and observing the results obtained in the last work it's possible to see that the sensors are also considerably more resistive. The problem that this grade is not commercialized anymore by Clevios™, which rendered the use this grade of PEDOT:PSS impossible in this work.

According to the analysis of the data given by the manufacturer, it's possible to see that both of the grades have almost the same characteristics, differing only in the viscosity and in the conductivity [55]. The other important parameters such as the proportion between PEDOT and PSS in solution or the particle size are the same [55]. It's known that one of the most important steps to achieve highly conductive polymers is the secondary doping. This is possibly the difference between this solutions, since they can be doped by different dopants and by different processes [55]. The increase of conductivity by the addition of secondary dopants it's explained by a phase separation of the PSS in excess in solution [72]. Normally the PSS counterions due to electrostatic forces are responsible to keep a certain space between PEDOT chains. The addition of PSS normally increases the separation of the PEDOT chains and consequently the decreases the conductivity of the polymer [73]. Due to phase separation of PSS the insulator influence of PSS is reduced and therefore the conductivity rises. It is also known that the pristine PEDOT:PSS solutions, without secondary dopants, reacts considerably to humidity due to a swelling process, when compared to secondary doped PEDOT:PSS solutions [55]. In sum, one possible explanation for the lack of sensitivity of the grade used in this work, when compared to the grade used in the last work, is the importance of the PSS behavior in the solution. A less

45

conductive polymer as PH1000, is less influenced by the swelling process of PSS after interaction with other molecules and therefore is less sensitive to other gases and relative humidity.

Another important and positive conclusion, is that all the sensors which were tested in this work independently of their geometrical characteristics, thicknesses and the analysis mode (resistive or capacitive), reacted to the presence of both gynecological analytes. However, it was also seen that it seems very difficult to distinguish both analytes. For the purposes of this work, it can be a problem since it should be important to distinguish a normal and healthy vaginal environment from an infected one.

The vaginal fluid simulators in this work had a different concentration of lactobacillus in the solution. Both of these analytes, are not very volatile aqueous solutions and have a big volume of water. This was proven to be problematic since the sensors exhibited a big sensitivity to the water and in fact in most of the cases it was very difficult to distinguish, not only the reaction of the sensors to both vaginal fluids but also to the water. So that, it can be concluded that the sensors developed in this work are very sensitive to the water, which can difficult the distinction of the analytes which have a big volume of water. The sensitivity of this type of sensors to the water is definitely an important parameter to take into account, since it means that the behavior of these sensors is very dependent on the relative humidity. Considering the fact that the vagina is an organ with more than 90% characteristic relative humidity is possible to conclude that the sensitivity of these sensors need to be studied with detail in the future and a new experimental setup needs to be developed for that purpose.

It was shown that it seems very difficult to distinguish the vaginal fluids from each other with different sensors of the same type, mainly because the differences between different sensors' response and the results' fluctuation linked to the instability of the experimental setup are higher than the sensor's sensitivity to these analytes. However, with only one sensor it was proven that not only it's possible to distinguish water from the vaginal analytes, that it's clear that the sensors react differently to the analytes with a clear pattern. This pattern suggests that the sensors react highly to the presence of water molecules than to the analytes. It is also possible to notice that the resistance and capacitance increase more healthy vaginal fluid which has 20 % less concentration of lactobacillus than the infected vaginal fluid. By the other hand, and considering the typical fluids from human mucosal, that is almost composed by several microorganisms in a water environment, a simple unbalance on such mucosal, must be ascribed to a possible pathogenic action. Taking into account the response of the organic electronic noses to the water, a change in such element due a disease can be naturally undirected detected. In the particular case of the actual work, the lactobacillus can be effectively detected. Some other gynecological diseases has a more "alcoholic" base elements and, once again, the present work can also show the possible detection. Considering an application in home care idea, and, after a correct calibration of the water dependent baseline, a simple, cheap and useful method can be achieved. Of course this undirected way for detection does not exclude the pathogenic agents directed detection as previously results have showed. For a more quantitative analysis (for instance in a clinical environment) the solution the solution is always a set of sensors, each one with different polymer (and therefore different reaction) where later the data are statistically analyzed.

In the present work, new interdigitated microelectrode's geometries were tested. It is clear from the results that different geometries have a big influence in the sensor's capacitive response. In the case of the circular and hexagonal geometries, the sensor showed in some cases different dynamics and sensitivities. At the same time, these geometries have a negative influence in the reproducibility of the sensor since the response for hexagonal and circular geometries can vary significantly from sensor to sensor. However, it's possible to conclude that the influence of the geometry seems an important factor to explore in the future since in some cases the one sensor can clearly distinguish the gynecologic fluids.

Three different thicknesses of the PEDOT:PSS were printed over the electrodes. Sensors of the same geometry with different thickness were studied and interesting results were observed. The results,

showed that there is a variation on the sensor's response for different thicknesses in both resistive and capacitive modes. While in the resistive mode it seems that the response of the sensors to the analytes is higher for thinner sensors, the inverse behavior happens when sensors are tested in the capacitive mode. Since only three different thicknesses were tested, it is difficult to describe the influence of the thickness in the effectiveness of the sensors. However, it seems that the influence is not linear. For the resistive mode thicker sensors (382,46 nm) have the poorest reaction. Sensors with intermediate (315,22 nm) and smaller (217,2 nm) thicknesses have higher reaction when compared to thicker sensors, but a similar reaction when compared with each other. Since the inverse behavior is observed for the capacitive mode, it seems that in this case the best choice of thickness is the intermediate one, which exhibits maximum effectiveness in response for the capacitive and the resistive mode.

New interdigitated electrodes with different geometrical parameters were also printed. The variation of parameters such as width, length and number of fingers, seem not to have considerable influence in the sensor's behavior. However, it is clear that the variation of geometrical parameters such as the gap width and the fingers' width influences considerably the resistive and the capacitive response. The results show that the higher the proportion between G and e the higher is the resistive response. From the other side, the smaller is this proportion, the higher is the capacitive response. This variation can be very useful, since for different applications may be more useful to use the capacitive or the resistive mode and in that case it's possible to choose the best parameters for the sensors.

The test with blue cheese showed also very promising results. The sensors exhibited considerably different sensitivities for a good cheese and for a spoiled cheese. These differences are big enough to be easily detected by a simple electronic system. Therefore, it's was proven the incredible potential of these sensors which can be used in many different area such as food spoilage.

Another very important remark to be done, is that in the resistive mode the sensors reacted with an increase of resistance when they were subjected to an analyte contaminated for a gynecological pathology. This pathology has a bacteriologic origin and is detected by the augmentation of the presence of lactobacillus in the vaginal fluid. In the previous work, a fungal culture of Candida was used as an analyte and the sensor with the same polymer had completely inverse response in the resistive mode since in that case, the analyte decreased the resistance of the sensor. This results can be very promising, since it's known that the symptoms of vaginal candidiasis are very similar to the symptoms of this bacteriologic disease. If the same inverse reaction is exhibited with the sensors developed in this work, it means that with a single sensor it may be possible in the future to distinguish vaginal candidiasis and bacteriological diseases which have completely different origin and consequently different treatment.

Future work:

This work showed a lot of potential for this sensors, but there is still a long process on the way to improve, not only the process of development,t but also the experimental setup and the response analysis. As it was mentioned before, a new experimental setup is needed. In the new experimental setup, the humidity inside the analysis chamber needs to be controlled and a new system of transfer of air needs to be planned.

Other commercial grades of PEDOT:PSS needs to be tested in order to try to find a grade with the same sensitivity as the PEDOT:PSS 500 used in the previous work. Another alternative is to develop new solutions and optimize a solution which reaches the best level of response.

It's seems possible the need to use the combination of more sensors with different sensitivities to build an e-nose capable of detecting with correct precision different analytes, so it will be crucial in the future to test different polymers such as PANI or POMA.

A deeper study on the influence of the geometric parameters of the IMs and for the different thicknesses of polymer film should be done in order to a have a precise understanding about the influence of such parameters in the sensors electrical response.

Atomic fore microscopy (AFM) and AFM-CS (Atomic force microscopy-current sensing) should also be done to the sensors, in order to characterize morphologically the surface of the polymers and also understand the modifications of the bulk conductivity before, during and after the exposition to the analytes.

Finally, the same type of sensors should be tested to a Candida culture and at the same type to the same analytes used in this work to confirm the possibility of the an easy distinction of bacteriologic and fungal gynecological diseases with only one sensor which could be an extremely important step to the development and future commercialization of these type of sensors.

5. References

[1]   M. S. Cosio, M. Scampicchio, and S. Benedetti, "Electronic Noses and Tongues," *Chem. Anal. Food Tech. Appl.*, pp. 219–247, 2012.

[2]   A. D. Wilson and M. Baietto, "Advances in electronic-nose technologies developed for biomedical applications," *Sensors*, vol. 11, pp. 1105–1176, 2011.

[3]   "Biossensores de odor para deteção de patologias ginecológicas," Universidade de Aveiro, 2014.

[4]   "CeNTI." [Online]. Available: http://www.centi.pt/. [Accessed: 30-Oct-2015].

[5]   T. Y. Dn and T. Yyepg, "TeAM YYePG," in *Analysis*, 2005.

[6]   J. Fraden, "Chemical Sensors," in *Handbook of Modern Sensors: Physics, Designs, and Applications*, 4th ed., Springer, Ed. 2010.

[7]   H.Patel, "Odor," in *The Electroninc Nose: Artificial Olfaction Technology*, 2014.

[8]   T. C. P. Susan S. Schiffman, "Introduction to Olfaction: Perception, Anatomy, Physiology, and Molecular Biology," in *Handbook of Machine Olfaction: Electronic Nose Technology*, 2006.

[9]   *Handbook of Machine Olfaction: Electronic Nose Technology.* 2006.

[10]   H. K. Patel, *The Electronic Nose: Artificial Olfaction Technology.* 2014.

[11]   F. J. Heredia, M. L. González-Miret, a. J. Meléndez-Martínez, and I. M. Vicario, *Instrumental Assessment of Food Sensory Quality.* Woodhead Publishing Limited, 2013.

[12]   J. M. Young and B. J. Trask, "The sense of smell: genomics of vertebrate odorant receptors," *Hum. Mol. Genet.* , vol. 11 , no. 10 , pp. 1153–1160, May 2002.

[13]   J. Gutiérrez and M. C. Horrillo, "Advances in artificial olfaction: Sensors and applications," *Talanta*, vol. 124, pp. 95–105, 2014.

[14]   Iowa State University, "Odor perception and physiological response.," *Sci. Smell*, vol. 1, no. May, p. 4, 2004.

[15]   G. Korotcenkov and B. K. Cho, "Engineering approaches for the improvement of conductometric gas sensor parameters: Part 1. Improvement of sensor sensitivity and selectivity (short survey)," *Sensors Actuators, B Chem.*, vol. 188, pp. 709–728, 2013.

[16]   Gutierrez-Osuna, R.Nagle, H. Troy, B. Kermani, and S. S. Schiffman, "Signal Conditioning and Preprocessing," in *Handbook of Machine Olfaction: Electronic Nose Technology*, Wiley-VCH Verlag GmbH & Co. KGaA, 2003.

[17]   E. L. Hines, P. Boilot, and J. W. G. and M. A. Gongora, "Pattern Analysis for Electronic Noses," in *Handbook of Machine Olfaction: Electronic Nose Technology*, Wiley-VCH Verlag GmbH & Co. KGaA, 2003.

[18]   H. Nanto and J. R. Stetter, "Introduction of chemosensors," in *Handbook of Machine Olfaction: Electronic Nose Technology*, Wiley-VCH Verlag GmbH & Co. KGaA, 2003.

[19]   G. Korotcenkov, "Metal Oxides," in *Handbook of Gas Sensor Materials*, 2014.

[20]   H.Patel, "Sensor used in E-nose," in *The Electronic Nose: Artifitial Olfaction Technology*, 2014.

[21]   G. Korotcenkov, "Materials for specific gas sensors," in *Handbook of Gas Sensor Materials*, 2014.

[22]   G. Korotcenkov, "Nanostrucutred Gas Sensing Materials," in *Handbook of Gas Sensor Materials. V2*, 2014.

[23]   G. Korotcenkov, "Nanocomposites," in *Handbook of Gas Sensor Materials. V2*, 2014.

[24]   O. a. Loaiza, P. J. Lamas-Ardisana, L. Añorga, E. Jubete, V. Ruiz, M. Borghei, G. Cabañero, and H. J. Grande, "Graphitized carbon nanofiber–Pt nanoparticle hybrids as sensitive tool for preparation of screen printing biosensors. Detection of lactate in wines and ciders," *Bioelectrochemistry*, vol. 101, pp. 58–65, 2015.

[25]   E. Llobet, "Gas sensors using carbon nanomaterials: A review," *Sensors Actuators, B Chem.*, vol. 179, pp. 32–45, 2013.

[26]   Rajesh, T. Ahuja, and D. Kumar, "Recent progress in the development of nano-structured conducting polymers/nanocomposites for sensor applications," *Sensors Actuators, B Chem.*, vol. 136, pp. 275–286, 2009.

[27]   R. Leghrib, T. Dufour, F. Demoisson, N. Claessens, F. Reniers, and E. Llobet, "Gas sensing properties of multiwall carbon nanotubes decorated with rhodium nanoparticles," *Sensors Actuators, B Chem.*, vol. 160, no. 1, pp. 974–980, 2011.

[28]   S. Chiu, J. Wang, G. Lin, C. Chang, H. Chen, and K. Tang, "Towards a Fully Integrated Electronic Nose SoC," pp. 166–169, 2012.

[29]   R. Dutta, E. L. Hines, J. W. Gardner, and P. Boilot, "Bacteria classification using Cyranose 320 electronic nose.," *Biomed. Eng. Online*, vol. 1, p. 4, 2002.

[30]   E. Westenbrink, R. P. Arasaradnam, N. O'Connell, C. Bailey, C. Nwokolo, K. D. Bardhan, and J. a Covington, "Development and application of a new electronic nose instrument for the detection of colorectal cancer," *Biosens Bioelectron*, pp. 1–6, 2014.

[31]   H.Patel, "Applications of Machine Olfaction," in *The Electronic Nose: Artifitial Olfaction Technology*, 2014.

[32]   I. a. Casalinuovo, D. Di Pierro, M. Coletta, and P. Di Francesco, "Application of Electronic Noses for Disease Diagnosis and Food Spoilage Detection," *Sensors*, vol. 6, pp. 1428–1439, 2006.

[33]   J. Paul and H. Lima, "Um nariz eletrônico baseado em polímeros condutivos," 2010.

[34]   S. Cui, J. Wang, L. Yang, J. Wu, and X. Wang, "Qualitative and quantitative analysis on aroma characteristics of ginseng at different ages using E-nose and GC–MS combined with chemometrics," *J. Pharm. Biomed. Anal.*, vol. 102, pp. 64–77, 2015.

[35]   L. Gil-Sánchez, J. Soto, R. Martínez-Máñez, E. Garcia-Breijo, J. Ibáñez, and E. Llobet, "A novel humid electronic nose combined with an electronic tongue for assessing deterioration of wine," *Sensors Actuators, A Phys.*, vol. 171, pp. 152–158, 2011.

[36]   A. D. Corrado Di Natale, Roberto Paolesse, "Food beaverage quality assurance," in *Handbook of Machine Olfaction: Electronic Nose Technology*, WILEY-VCH Verlag GmbH & Co. KGaA, 2003.

[37]   X. Hong, J. Wang, and G. Qi, "E-nose combined with chemometrics to trace tomato-juice quality," *J. Food Eng.*, vol. 149, pp. 38–43, 2015.

[38]   Ł. Guz, G. Łagód, K. Jaromin-Gleń, Z. Suchorab, H. Sobczuk, and A. Bieganowski, "Application of Gas Sensor Arrays in Assessment of Wastewater Purification Effects," *Sensors*, vol. 15, no. 3, pp. 1–21, 2014.

[39]   S. S. S. H. Troy Nagle, Ricardo Gutierrez-Osuna, Bahram G. Kermani, "Environmental Monitoring," in *Handbook of Machine Olfaction: Electronic Nose Technology*, 2003.

[40]   O. Canhoto and N. Magan, "Electronic nose technology for the detection of microbial and chemical contamination of potable water," *Sensors Actuators, B Chem.*, vol. 106, pp. 3–6, 2005.

[41]   V. K. Pamula, "Detection of Explosives," in *Handbook of Machine Olfaction*, Wiley-VCH Verlag GmbH & Co. KGaA, 2004, pp. 547–560.

[42]   P. A. Rodriguez, T. T. Tan, and H. Gygax, "Cosmetics and Fragrances," in *Handbook of Machine Olfaction*, Wiley-VCH Verlag GmbH & Co. KGaA, 2004, pp. 561–577.

[43]   M. A. Ryan and H. Zhou, "Automotive and Aerospace Applications," in *Handbook of Machine Olfaction*, Wiley-VCH Verlag GmbH & Co. KGaA, 2004, pp. 525–546.

[44]   T. Kenny, *Sensor Technology Handbook*. Elsevier, 2005.

[45]   A. J. Epstein, "Electrical Conductivity in Conjugated Polymers," in *Conductive Polymers and Plastics in Industrial Applications*, Plastics Design Library, 1999, pp. 1–11.

[46]   A. J. Epstein, "Conducting Polymers: Electrical Conductivity," in *Physical Properties of Polymers Handbook*, vol. 199, Springer, 1997, pp. 725–752.

[47]   H. Bai and G. Shi, "Gas Sensors Based on Conducting Polymers," *Sensors*, vol. 7, pp. 267–307, 2007.

[48]   R. Balint, N. J. Cassidy, and S. H. Cartmell, "Conductive polymers: Towards a smart biomaterial for tissue engineering," *Acta Biomater.*, vol. 10, no. 6, pp. 2341–2353, 2014.

[49]   U. Lange, N. V. Roznyatovskaya, and V. M. Mirsky, "Conducting polymers in chemical sensors and arrays," *Anal. Chim. Acta*, vol. 614, pp. 1–26, 2008.

[50]   W. H. Grover, "Interdigitated Array Electrode Sensors: Their Design , Efficiency , and Applications," *Honor. thesis , Univ. Tennessee*, 199

[51]   M. S. A. Rahman, S. C. Mukhopadhyay, and P.-L. Yu, "Novel Sensors for Food Inspection: Modelling, Fabrication and Experimentation," in *Novel Sensors for Food Inspection: Modelling, Fabrication and Experimentation*, Springer, 2014.

[52]   N. Gupta, S. Sharma, I. A. Mir, and D. Kumar, "Advances in sensors based on conducting polymers," *J. Sci. Ind. Res. (India).*, vol. 65, no. 7, pp. 549–557, 2006.

[53]   G. Korotcenkov, "Polymers," in *Handbook of Gas Sensor Materials*, 2014, pp. 154–157.

[54]   W. S. Wong and A. Salleo, *Flexible Electronics: Materials and Applications Electronic Materials: Science and Technology*. 2009.

[55]   A. Elschner, S. Kirchmeyer, W. Lövenich, U. Merker, and K. Reuter, *PEDOT:Principles and Applications of an Intrinsically Conductive Polymer PEDOT*. Taylor and Francis Group, 2011.

[56]   O. Bubnova, "Thermoelectric properties of conducting polymers Thermoelectric properties of conducting polymers Olga Bubnova," Linköping University, 2013.

[57]   W. Lövenich, "PEDOT-properties and applications," *Polym. Sci. Ser. C*, vol. 56, no. 1, pp. 135–143, 2014.

[58]   M. I. Marques, J. Fonseca, J. Gomes, A. Palmeira-de-Oliveira, J. Martinez-de-Oliveira, and L. Pereira, "Organic Based Bio-sensor for Odor Detection in Gynecological Diseases," *Mater. Today Proc.*, vol. 2, no. 1, pp. 236–241, 2015.

[59]   S. Timpanaro, M. Kemerink, F. J. Touwslager, M. M. De Kok, and S. Schrader, "Morphology and conductivity of PEDOT/PSS films studied by scanning-tunneling microscopy," *Chem. Phys. Lett.*, vol. 394, pp. 339–343, 2004.

[60]   M.Nandakumar and A. Paramasivam, "Principles of Screen Printing Process," in *Gravure, Flexography & Screen Printing*, Department of Printing Technology Arasan Ganesan Polytechnic College, Sivakasi.

[61]   A. A. Tracton, "Screen Printing," in *Coatings Technology Handbook, Third Edition*, CRC Press, 2005.

[62]   S. Khan, L. Lorenzelli, R. Dahiya, and S. Member, "Technologies for Printing Sensors and Electronics over Large Flexible Substrates: A Review," *IEEE Sens. J.*, vol. PP, no. 99, 2014.

[63]   W. S. Wong and A. Salleo, *Flexible Electronics: Materials and Applications*. 2009.

[64]   A. A. Tracton, "Slot Die Coating for Low Viscosity Fluids," in *Coatings Technology Handbook*, Third Edit., CRC Press, 2005.

[65]   W. a Maryniak, T. Uehara, and M. a Noras, "Number 1005 Surface Resistivity and Surface Resistance Measurements Using a Concentric Ring Probe Technique Trek Application Note Number 1005 Surface Resistivity and Surface Resistance Measurements Using a Concentric Ring Probe Technique," no. 1005, pp. 1–4, 1804.

[66]   J. Pitkin, A. B. Peattie, and B. A. Magowan, *Also available*, vol. 1, no. 60. CHURCHILL LIVINGSTONE, 2003.

[67]   D. H. Owen and D. F. Katz, "A vaginal fluid simulant," *Contraception*, vol. 59, no. 2, pp. 91–95, 1999.

[68]   "http://www.rokuprint.com/eng/debgcms/cmsdata/artikel/144/db_rp_2.2_e.pdf." [Online]. Available: http://www.rokuprint.com/eng/debgcms/cmsdata/artikel/144/db_rp_2.2_e.pdf. [Accessed: 25-Apr-2015].

[69]   M. F. Mabrook, C. Pearson, and M. C. Petty, "Inkjet-printed polymer films for the detection of organic vapors," *IEEE Sens. J.*, vol. 6, no. 6, pp. 1435–1443, 2006.

[70]   G. Gillot, J. Jany, M. Coton, G. Le Floch, S. Debaets, J. Ropars, M. López-villavicencio, J. Dupont, and A. Branca, "Insights into Penicillium roqueforti Morphological and Genetic Diversity," *PLoS One*, vol. 10, no. 6, 2015.

[71]   "microFLEX." [Online]. Available: http://3d-micromac.com/products/microflex/. [Accessed: 25-Apr-2015].

[72]   X. Crispin, F. L. E. Jakobsson, a Crispin, P. C. M. Grim, P. Andersson, a Volodin, C. van Haesendonck, M. Van der Auweraer, W. R. Salaneck, and M. Berggren, "The origin of the high conductivity of poly(3,4-ethylenedioxythiophene)-poly(styrenesulfonate) (PEDOT- PSS) plastic electrodes," *Chem. Mater.*, vol. 18, no. 4, pp. 4354–4360, 2006.

[73]   M. Kuş and S. Okur, "Electrical characterization of PEDOT:PSS beyond humidity saturation," *Sensors Actuators, B Chem.*, vol. 143, no. 1, pp. 177–181, 2009.